# TWO-PHASE FLOW REGIME TRANSITIONS UNDER A D.C. ELECTRIC FIELD

Part A

# TWO-PHASE FLOW REGIME TRANSITIONS UNDER A D.C. ELECTRIC FIELD

by

K.S. BRUNNER, B.Sc.

On-Campus Report

Submitted to the School of Graduate Studies

in Partial Fulfillment of the Requirements

for the Degree

Master of Engineering

McMaster University

July 1981

MASTER OF ENGINEERING (1981)
ENGINEERING PHYSICS

MCMASTER UNIVERSITY
Hamilton, Ontario.

TITLE; Two-Phase Flow Regime Transitions Under a D.C. Electric Field

AUTHOR: K.S. Brunner, B.Sc.,

NUMBER OF PAGES: vii, 58,A11

## ABSTRACT

The air-water flow regime transitions in a horizontal pipe under the influence of a strong electric field perpendicular to the interface are studied. The separated flow model to predict flow regime transitions has been developed. The present version of the model is a modification of Taitel and Dukler's separated flow model. This assumes that all flow regimes are perturbations from stratified smooth flow. Expressions for the electrical force are derived and added to the conservation and constitutive equations to obtain new transition criteria. The theoretical results are compared with observations of air-water flow in a 1.27 cm. and 1.9 cm. internal diameter pipe. Good agreement was found when no electric field was applied, however, the experimentally observed effect of the electric field was not as pronounced as predicted by theory. Further experiments to refine the theoretical model are presented.

## ACKNOWLEDGEMENTS

The author gratefully acknowledges the supervision of Dr. J.S. Chang for this report. I would also like to thank Mr. R. Girard, and Mr. J. Montgomery for their suggestions on experimental apparatus.

TABLE OF CONTENTS

## List of Illustrations

## List of Tables

# CHAPTER 1

## Introduction

It is well known that an electric field will enhance heat transfer, particularly in the boiling regime (Figure 1.0.1). As a result there are many instances where an electric field is applied to a two-phase system to increase heat transfer. Even though much work has been done in applying an electric field to a pool boiling system, little has been done with flow in pipes. The situation in pipes will be a little more complex than simple pool boiling as the electric field will also affect the flow. This work attempts to isolate the effect of the electric field on the flow by examining a simple case of horizontal gas-fluid flow through a vertical electric field.

### 1.1 Electro-hydro-dynamic Heat Transfer

Much work, both experimental and theoretical, has been done on the increased transfer of heat to fluids under the influence of non-uniform electric fields. (Mascarenhas, 1957; Ashmann and Kronig, 1949, 1951; Bonjour, et al., 1962; Johnson, 1968; Lovenguth and Hanesian, 1971; Markels and Durfee, 1964). Increases in heat flux by a factor of ten have been reported, apparently limited only by the applied voltage. The mechanism of increased heat flux varies depending on the type of heat transfer involved. With convective heat transfer there is an increase in convection due to the electric force (EHD flow). The electric force

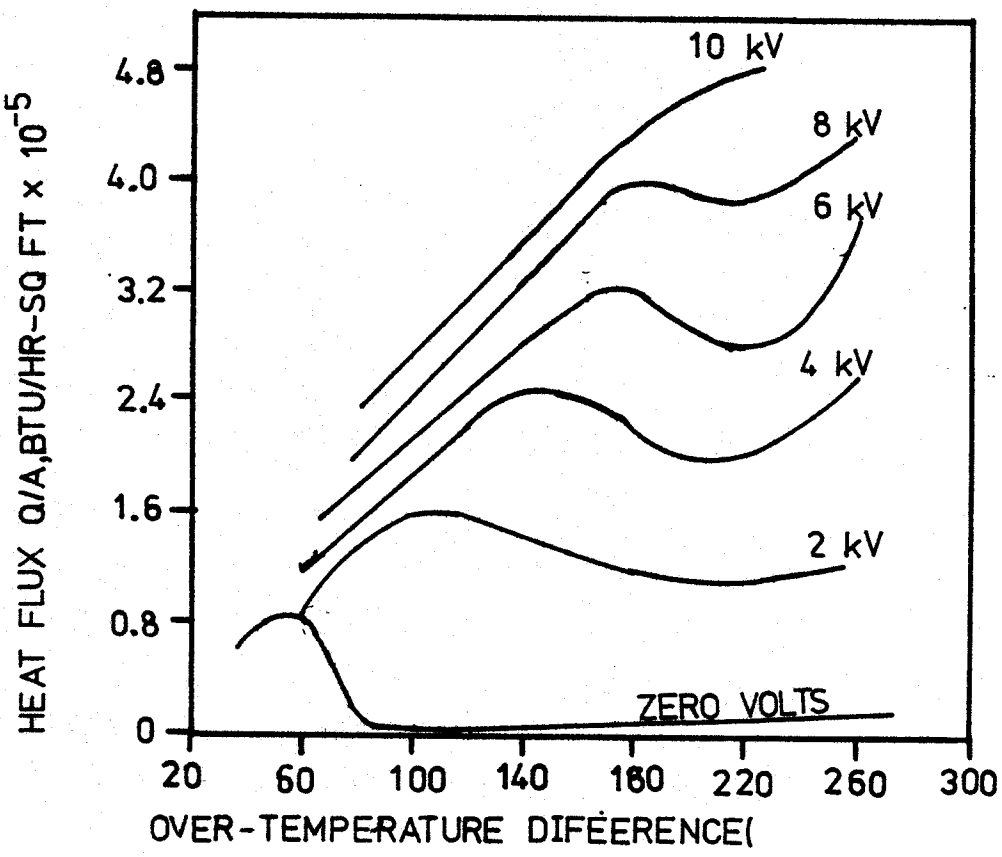


FIGURE I.O.I: EFFECT OF D.C. VOLTAGE ON POOL BOILING HEAT TRANSFER(FROM MARKELS AND DURFEE, 1964)

is caused by different dielectric susceptibilities due to temperature differences in the nonconducting fluid (Kronig and Ashmann, 1951). Conduction can also play a major role giving a vastly increased heat transfer even at low electric fields (Mascarenhas, 1957).

The nucleate boiling regime consists of jets of vapour flowing outwards interspersed with jets of fluid flowing inwards. The jets are stable until a certain velocity differential is reached, after which they break up and film boiling sets in. The electric field enhances the heat flux by allowing larger jets and increased vapour and liquid flows. It acts as a stabilizing influence on the vapour-liquid interface (Johnson, 1967).

Several possible applications may be found for increased heat transfer under an electric field. The efficiency of boilers may be enhanced by this effect, as well as condenser efficiency. The cooling systems of high power transformers are immersed in transformer oil to cool them. An increased heat transfer would allow smaller transformers to carry the same power load (Aihara, 1967).

Other applications can occur almost anywhere high voltages and cooling are needed. Cooling of transmission lines (Tahaka and Kurbo, 1977, Watabe, Kibudu and Yokoyama, 1979) and high power transistors (Fujii, 1978) are two such applications. If there is a small break in the pressurized cooling system, voiding will occur. The amount of coolant loss is dependent on the pressure drop, and this in turn depends on the flow regime (Wallis and Dobson, 1973; Taitel and Dukler, 1976).

Even though an applied electric field will increase heat transfer in a heat exchanger such as a boiler or condenser, nothing is known about the effect of the electric field on the flow patterns inside the heat exchanger. Many of the applications noted above utilize boiling cooling, as well as convective cooling. Here, the flow regime will play a major part in the heat transfer mechanism as it will govern the rewetting of the pipes.

The sudden electrical impulse caused by lightning striking a pipe could result in an electric field being formed in the pipe. If this affects the flow regime sudden pressure surges could cause the pipe to rupture, or result in serious disruption of the flow, since it has been found that the flow regime has a large effect on the pressure drop in a pipe (Wallis and Dobson, 1973; Taitel and Dukler, 1976).

## 1.2 Flow Regimes in Horizontal Gas-Fluid Flow

During horizontal, cocurrent gas-fluid flow in pipes, a number of flow patterns, normally called regimes, are found to exist. These result from the particular manner in which the gas-fluid flow is distributed in the pipe. Even though most authors define flow regimes somewhat differently, most agree on six different flow regimes. These are shown in Figure 1.2.1.

The following definitions will be the ones used in this paper. Stratified smooth (SS) flow occurs when the fluid is at the bottom of the pipe and the gas flows along the top. The surface of the fluid is smooth. Stratified wavy (SW) flow is similar to stratified smooth,

however the gas-fluid interface is wavy instead of smooth. Both elongated bubble (EB) (this is also designated as plug flow) and slug (S) flow, are what Taitel and Dukler call intermittent flow. This flow regime is characterized by the fluid bridging the gap between the gas-fluid interface and the top of the pipe. The difference between slug and plug flow depends on the degree of agitation of the bridge. This work follows the definition of Taitel et al., 1979. Plug flow is considered to be the limiting case of slug flow where no entrained bubbles exist in the fluid slug.

Annular (A) flow occurs when the walls are wet by a thin film of fluid while gas at high velocity flows through the centre of the pipe. Fluid droplets are usually entrained in this gas. When the upper walls are intermittently wet by large aerated waves sweeping through the pipe it is not slug flow, which requires a complete fluid bridge, nor annular flow which requires a stable film. Again following Taitel et al., 1979, this has been designated as wavy annular (WA) flow. This flow regime was not recognized by Mandhane et al., 1974, and was considered to be slug flow.

The last regime is the dispersed bubble (DB) or bubbly regime. The fluid completely fills the pipe while small gas bubbles are distributed throughout the body of the pipe. The transition to this regime is characterized by the gas bubbles losing contact with the top of the pipe. At first the bubbles are near the top of the pipe, but become more uniformly distributed at higher liquid flow rates.

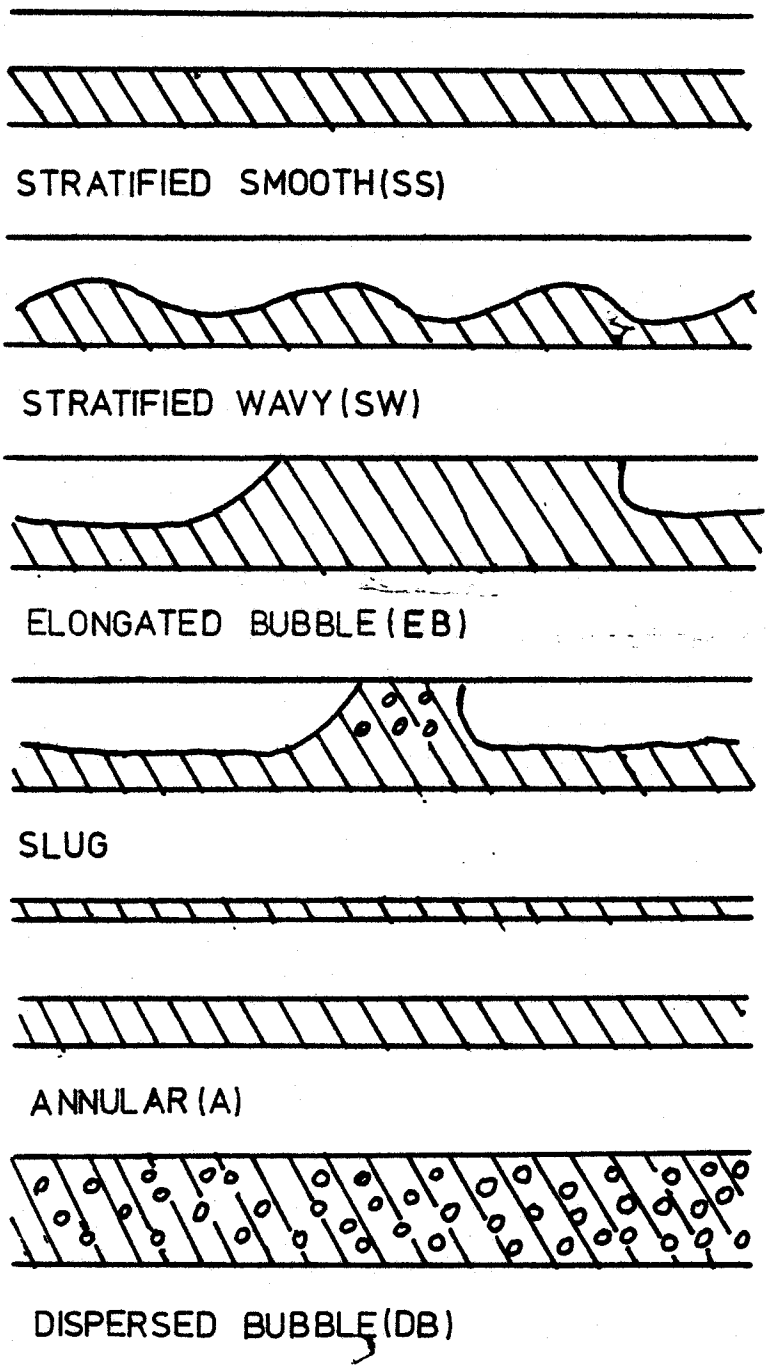


FIGURE 1.2.1: FLOW REGIMES IN TWO-PHASE HORIZONTAL FLOW

## 1.3 Previous Work on Flow Regime Mapping in Horizontal Flow

Original attempts to predict the flow regime in a horizontal pipe were done with empirical maps, the two most well known being that of Baker, 1954; and Mandhane et al., 1974. These were maps which attempted to correlate the results of many experiments using different sized pipes. These maps are shown in Figures 1.3.1 and 1.3.2. In the Baker map, $\lambda = [(\rho_g/0.075)(\rho_f/62.3)]$; $\psi = [(73/\sigma)\mu_f(62.3/\rho_f)^2]^{1/3}$; $\rho_g, \rho_f$ in lb/ $ft^3$; $G_g$, $G_f$ in lb/hr.$ft^2$; $\sigma$ in dyne/cm; $\mu_f$ in centipoise. In the Mandhane map only the gas and fluid specific velocities are used to correlate the flow regime transitions. This is because the map of Mandhane et al. is only applicable to air-water flow. A problem with both maps is that they are applicable only to horizontal flow, and do not adequately account for the effect of pipe size.

Kordyban and Ranov, 1970, were among the first to consider the mechanisms behind the flow regime transitions. They dealt with the stratified and stratified wavy to slug transition in a rectangular channel. The onset of slugging was considered to be a result of a Kelvin-Helmholtz instability in the interface causing the amplitude of the wave to increase until it touches the top of the channel. However, their theoretical predictions depended on measurement of the wavelength in stratified wavy flow, and so was not completely predictive.

Wallis and Dobson, 1973, also considered the transition to slug flow in a rectangular channel. Like Kordyban and Ranov, they considered slug formation to be a Kelvin-Helmholtz instability. By assuming the wavelength is "long" (compared to the amplitude of the wave), they eliminated wavelength from the equation and derive an expression in

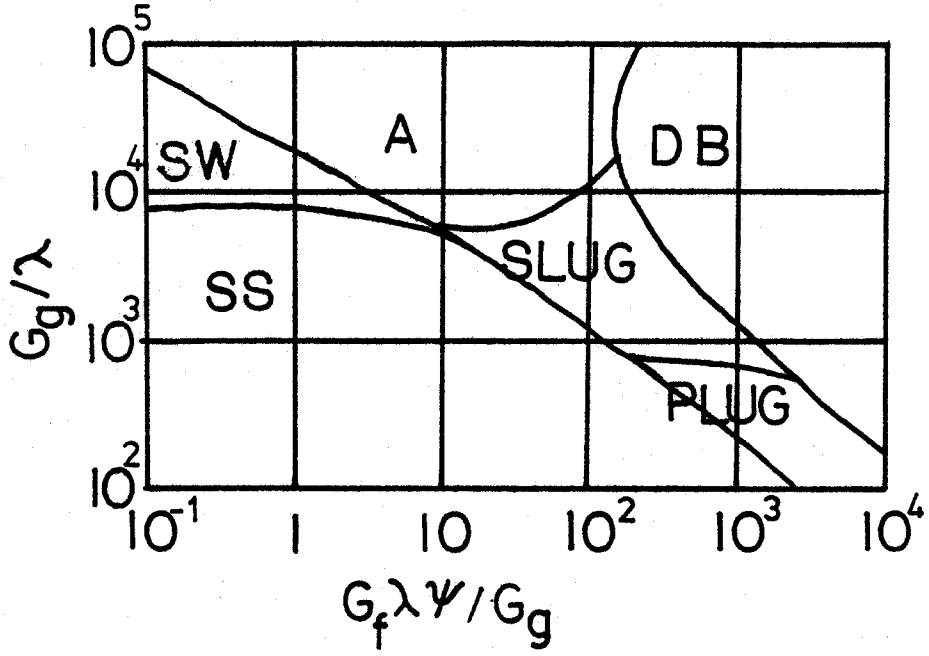


FIGURE 1.3.1: BAKER FLOW REGIME MAP

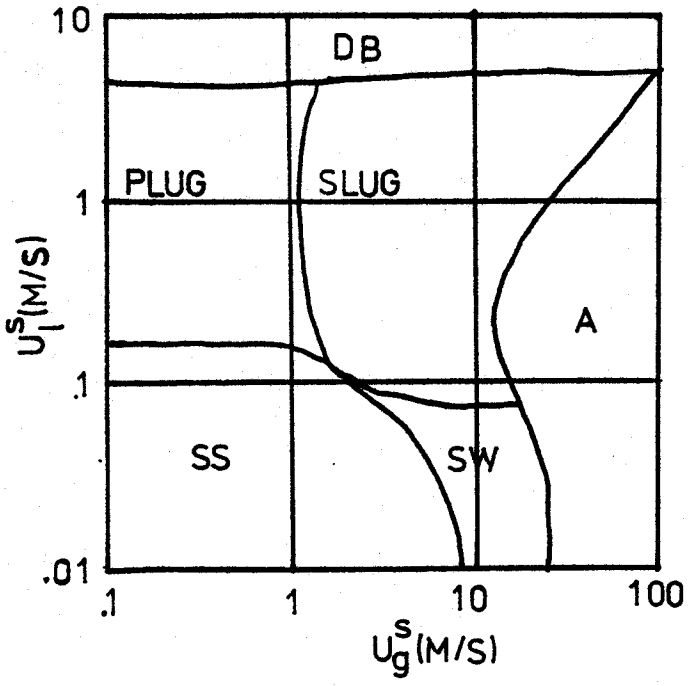


FIGURE 1.3.2: FLOW REGIME MAP OF MANDHANE ET AL.

terms of volumetric flow rates only. This gives good results, but is not applicable to a circular pipe. Also, in the experiments the gas-fluid interface was set parallel to the bottom of the channel. As a result the channel was tilted making it difficult to make any comparisons with a completely horizontal pipe. It is highly unlikely that a real-life situation with the pipe tilted in such a manner can arise, so the results are of limited applicability.

Taitel and Dukler, 1976, were the first to deal with more than one transition. Their basic assumption is that all flow regimes can be regarded as a deviation from stratified smooth flow, it being well established that the existence of a specific flow pattern at given gas and fluid flow rates is independent of the path used to arrive at that state.

Their starting point therefore, was to develop a relationship between flow rates and fluid level for stratified flow. This was done by equating pressure drop in the fluid to that in the gas.

This height was then used to define transitions to wavy, intermittent (this includes slug and elongated bubble flow), annular, and dispersed bubble flow regimes in the form of dimensionless constants.

Their method had several advantages. It could define a complete flow regime map. Only the volumetric flow rates of the fluid and gas are needed to predict the flow regime, and this method can be used to predict flow regimes in small inclined pipes as well. The disadvantage is that it doesn't take properties such as viscosity and surface

tension adequately into account. However, the flow regimes are predicted fairly accurately for an air-water system.

Further work has been done by Choe et al., 1978, and Weisman et al., 1979. Both use semiempirical correlations to decrease the data scatter for flow transitions. Both take the surface tension and fluid viscosity into account. This was proven to be necessary as Weisman et al., 1979 found significant transition variation with variations in these properties.

Gardner, 1979, has further treated the stratified to slug transition by balancing the energy and momentum flows at the trough and crest of the wave. This does better than Taitel and Dukler, 1976, at predicting the transition to slug flow, but the wave height is needed to predict the flow rates. Thus Gardner's theory is not completely predictive.

The approach of Taitel and Dukler, 1976, has been selected as the basis for the present work as it is the only approach which models all flow regime transitions. Moreover, it is completely predictive, needing only the gas and fluid flow rates to determine the regime. This reduces the number of measurements necessary. Finally, the model, although not as good as some, gives very good results for the air-water system which will be used for experiments.

# CHAPTER 2

# Theory

## 2.1 The Electrical Force

As mentioned in the introduction the basic theoretical model used to predict the effect of an applied electric field on flow regime transitions is the separated flow model. The separated flow model of Taitel and Dukler, 1976, is modified by introducing an extra force due to an applied electric field. The first step therefore is to examine the nature of this force (often called the "pondero-motive" force).

The first problem encountered is that the system will be an air-water system. Although air can be considered as an insulator, the exact properties of water are not known as they depend on the local water conditions. Therefore, the water is considered both as a dielectric (distilled water) as well as a conductor in the present model.

In the present separated flow model the stratified flow system is considered as the "basic" system. Therefore, the force of a uniform electric field perpendicular to the air-water interface is found.

The situation is shown in Figures 2.1.1 and 2.1.2, where $\varepsilon^{(1)}$ and $\varepsilon^{(2)}$ are the dielectric constants of the water and air respectively.

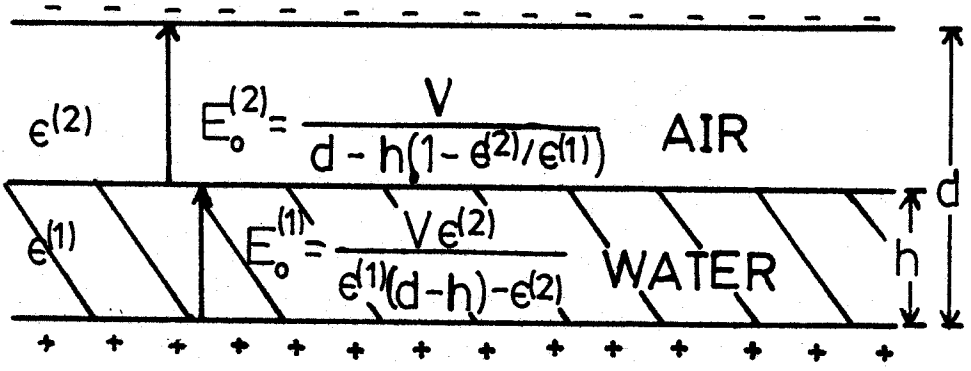


FIGURE 2.1.1 : ELECTRIC FIELDS WHEN WATER IS CONSIDERED AS A DIELECTRIC ( COMPLETELY DEIONIZED)

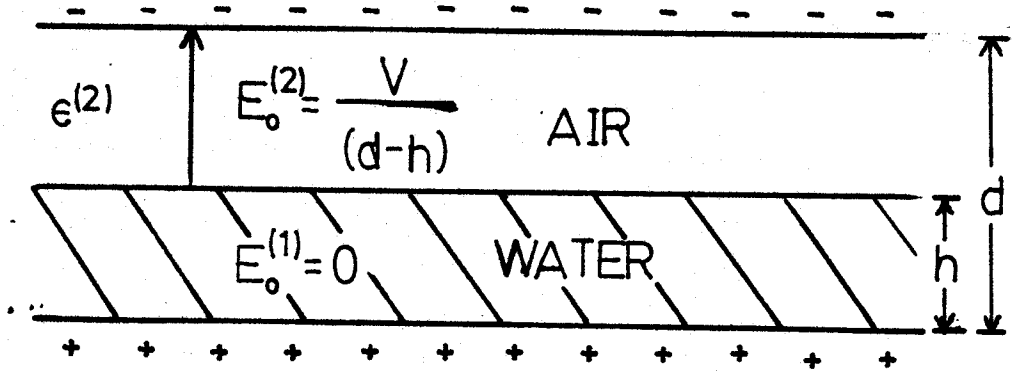


FIGURE 2.1.2: ELECTRIC FIELDS WHEN WATER IS CONSIDERED AS A CONDUCTOR (CONTAMINATED)

The force per unit area on the water surface can easily be found by energy considerations (Duffin, 1973). For water as a dielectric it is,

$$f_d = \frac{1}{2} (E^{(2)})^2 \varepsilon_o \varepsilon^{(2)} (1 - \varepsilon^{(2)}/\varepsilon^{(1)}) \quad (1)$$

For the conductor the expression becomes,

$$f_c = \frac{1}{2} \varepsilon^{(2)} \varepsilon_o (E^{(2)})^2 \quad (2)$$

In the present system the electric fields in the two different media are only dependent on the surface position and voltage, giving the expressions in Figures 2.1.1 and 2.1.2. Therefore, equations (1) and (2) become,

$$f_d = \frac{1}{2} \left( \frac{V}{d-h(1-\varepsilon^{(2)}/\varepsilon^{(1)})} \right)^2 \varepsilon_o \varepsilon^{(2)} (1-\varepsilon^{(2)}/\varepsilon^{(1)}) \quad (3)$$

$$f_c = \frac{1}{2} \left( \frac{V}{d-h} \right)^2 \varepsilon_o \varepsilon^{(2)} \quad (4)$$

In the present separated flow model (Taitel and Dukler, 1976), the analysis assumes that the wave is of finite height. As the electrical force is dependent on the position of the interface, the force will be different at the trough and the crest of the wave. Both forces act in the same direction, so it is the difference in force on the surface that is important. In this respect the electrical force is much like pressure. Consider a system with a wave trough at h and a crest at h'. This gives the following for the difference in forces,

$$\Delta f_d = \frac{1}{2}\left[\frac{V}{d - h'(1-\varepsilon^{(2)}/\varepsilon^{(1)})}\right]^2 \varepsilon_o\varepsilon^{(2)}(1-\varepsilon^{(2)}/\varepsilon^{(1)} - \frac{1}{2}\left[\frac{V}{d - h\ (1-\varepsilon^{(2)}/\varepsilon^{(1)})}\right]^2 \varepsilon_o\varepsilon^{(2)}(1 - \varepsilon^{(2)}/\varepsilon^{(1)}) \quad (5)$$

$$\Delta f_c = \frac{1}{2}\left[\frac{V}{d-h'}\right]^2 \varepsilon_o\varepsilon^{(2)} - \frac{1}{2}\left[\frac{V}{d-h}\right]^2 \varepsilon_o\varepsilon^{(2)} \quad (6)$$

The further simplifying assumption is made that the difference between h and h' is small compared to h. Now, letting $h' = h + \Delta h$ and using the appropriate expansions we obtain,

$$\Delta f_d = \frac{1}{2}\left[\frac{V}{d-h\ (1 - \varepsilon^{(2)}/\varepsilon^{(1)})}\right]^2\left[1 + \frac{2\Delta h\ (1 - \varepsilon^{(2)}/\varepsilon^{(1)})}{d-h\ (1 - \varepsilon^{(2)}/\varepsilon^{(1)})}\right] - \frac{1}{2}\left[\frac{V}{d-h\ (1-\varepsilon^{(2)}/\varepsilon^{(1)})}\right]^2 \varepsilon_o\varepsilon^{(2)}\ (1 - \varepsilon^{(2)}/\varepsilon^{(1)}) \quad (7)$$

$$\Delta f_c = \frac{1}{2}\left(\frac{V}{d-h}\right)^2\left(1 + \frac{2\Delta h}{d-h}\right)\varepsilon_o\varepsilon^{(2)} - \frac{1}{2}\left(\frac{V}{d-h}\right)^2 \varepsilon_o\varepsilon^{(2)} \quad (8)$$

This gives the following final form for the electrical force,

$$\Delta f_d = \frac{V^2}{[d-h\ (1 - \varepsilon^{(2)}/\varepsilon^{(1)})]^3}\ \varepsilon_o\varepsilon^{(2)}(1 - \varepsilon^{(2)}/\varepsilon^{(1)})^2\Delta h \quad (9)$$

$$\Delta f_c = \frac{V^2}{(d-h)^3}\ \varepsilon_o\varepsilon^{(2)}\Delta h \quad (10)$$

Note that the expression for the dielectric would become the same as that for the conductor if $\varepsilon^{(1)}$ is allowed to go to infinity. This corresponds to a conducting medium.

## 2.2 Liquid Level in Horizontal Stratified Flow

In the present model we assume all flow regimes to be perturbations from the horizontal stratified flow regime. The primary property of this regime is the liquid level. This is found by equating

the pressure drops in air and water and considering the momentum balance. Consider the cross-sectional planes shown in Figure 2.2.1. D is the pipe diameter, $h_L$ is the height of the liquid in the pipe, $A_G$ and $A_L$ are the gas and liquid cross-sectional areas respectively, $S_G$ is the gas perimeter, $S_L$ is the liquid perimeter and $S_i$ is the length of the interface between the two. In the second diagram $U_G$ and $U_L$ are the gas and liquid velocities, $\alpha$ is the angle of the pipe with the horizontal, E is the electric field and $\gamma$ is the angle of the electric field with the pipe.

Since the gas-fluid system is in equilibrium the total change in momentum for each system must be zero. This gives the following equations for the fluid and gas phases respectively,

$$-A_L \frac{dp}{dx} - \tau_{WL} S_L + \tau_i S_i + \rho_L A_L g \sin\alpha - S_i f_e \cos\gamma = 0 \qquad (11)$$

$$-A_G \frac{dp}{dx} - \tau_{WG} S_G - \tau_i S_i + \rho_G A_G g \sin\alpha + S_i f_e \cos\gamma = 0 \qquad (12)$$

where $\frac{dp}{dx}$ is the change in pressure along the pipe, $\tau_{WL}$ is the shear stress of the wall on the liquid, $\tau_{WG}$ is the shear stress of the wall on the gas, $\tau_i$ is the interfacial shear stress, $\rho_L$ and $\rho_G$ are the liquid and gas densities, $f_e$ is the electrical force evaluated as in eq'ns (9) + (10) and g is the gravitational acceleration.

Now the pressure drops in the two phases are equated. Negligible hydraulic losses are assumed giving

$$\tau_{WG} \frac{S_G}{A_G} - \tau_{WL} \frac{S_L}{AL} + \tau_i S_i \left[\frac{1}{AL} + \frac{1}{A_G}\right] + \left[\rho_L - \rho_G\right] g \sin\alpha$$

$$-2 S_i f_e \cos\gamma \left(\frac{1}{A_G} + \frac{1}{A_L}\right) = 0 \qquad (13)$$

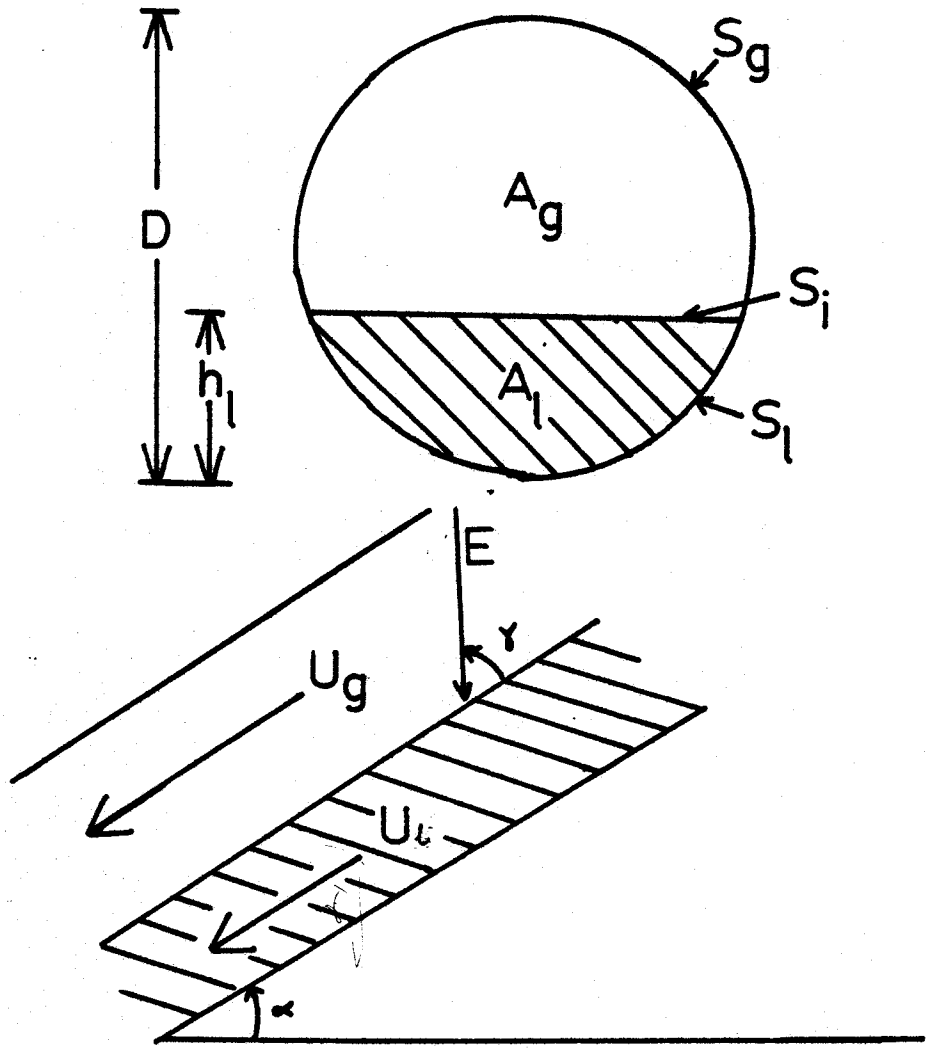


FIGURE 2.2.1 : GAS-LIQUID SYSTEM IN EQUILIBRIUM STRATIFIED FLOW

The shear stresses are evaluated in the usual manner, which is

$$\tau_{WL} = \frac{f_L \rho_L U_L^2}{2}, \quad \tau_{WG} = f_G \frac{\rho_G U_G^2}{2} \quad \tau_i = f_i \frac{\rho_G (U_G - U_L)^2}{2} \qquad (14)$$

The liquid and gas friction factors ($f_i$ and $f_G$) are evaluated as suggested by Agrawal et al., 1973,

$$f_L = C_L \left(\frac{D_L U_L}{\nu_L}\right)^{-n} \qquad f_G = C_G \left(\frac{D_G U_G}{\nu_G}\right)^{-m} \qquad (15)$$

where $D_L$, $D_G$ are the hydraulic diameters, and $\nu_L$, $\nu_G$ are the liquid and gas viscosities respectively. $C_G$, $C_L$, n and m are constants whose value depends on whether the flow is laminar or turbulent. The same values used by Taitel and Dukler, 1976, are applied, i.e. $C_G = C_L = 0.46$, $n = m = 0.2$ for turbulent flow, and $C_L = C_G = 1.6$, $n = m = 1.0$ for laminar flow.

The hydraulic diameters are also evaluated as suggested by Agrawal et al., 1973,

$$D_L = \frac{4A_L}{S_L} \qquad D_G = \frac{4A_G}{S_i + S_G} \qquad (16)$$

The shear stress due to stratified smooth flow has been shown to be approximately equal to the gas shear stress, so $f_i = f_G$, (Gazley, 1949). A slight error may occur with the present assumption as many of the transitions occur from the stratified wavy regime. However, from the estimation of Taitel and Dukler, 1976, this error is expected to be very small.

Since a general expression applicable to pipes of various sizes is wanted, it is useful to transform the equations to dimensionless form. The normalizing variables are: D for length, $D^2$ for area, and the superficial velocities $U_G^S$ and $U_L^S$ for the gas and liquid velocities. By combining equations (13) to (16), we obtain,

$$X^2 \left[ (\tilde{U}_L \tilde{D}_L)^{-n} \tilde{U}_L^2 \frac{\tilde{S}_L}{\tilde{A}_L} \right] - \left[ (\tilde{U}_G \tilde{D}_G)^{-m} \tilde{U}_G^2 \left( \frac{\tilde{S}_G}{\tilde{A}_G} + \frac{\tilde{S}_i}{\tilde{A}_L} + \frac{\tilde{S}_i}{\tilde{A}_G} \right) \right]$$

$$- 4Y - 4 S_i \left( \frac{1}{\tilde{A}_L} + \frac{1}{\tilde{A}_G} \right) Z = 0 \qquad (17)$$

where,

$$X^2 = \frac{\frac{4C_L}{D} \left( \frac{U_L^S D}{\nu_L} \right)^{-n} \frac{\rho_L (U_L^S)^2}{2}}{\frac{4C_G}{D} \left( \frac{U_G^S D}{\nu_G} \right)^{-m} \frac{\rho_G (U_G^S)^2}{2}} = \frac{\left| (dp/dx)_L^S \right|}{\left| (dp/dx)_G^S \right|} \qquad (18)$$

$$Y = \frac{(\rho_L - \rho_G)\, g \sin\alpha}{4 \frac{C_G}{} \left( \frac{U_G^S D}{\nu_G} \right)^{-m} \frac{\rho_G (U_G^S)^2}{2}} = \frac{(\rho_L - \rho_G) g \sin\alpha}{\left| (dp/dx)_G^S \right|} \qquad (19)$$

$$Z = \frac{2Df_e \cos\gamma}{\frac{4C_G}{D} \left( \frac{U_G^S D}{\nu_G} \right)^{-m} \frac{\rho_G (U_G^S)^2}{2}} = \frac{2Df_e \cos\gamma}{\left| (dp/dx)_G^S \right|} \qquad (20)$$

The dimensionless quantities are denoted by a tilde (~). The dimensionless variables in equation (17) can all be calculated with the dimensionless water level $\tilde{h}_L = h_L/D$ only, as follows,

$$\tilde{A}_L = 0.25\ [\pi - \cos^{-1}(2\tilde{h}_L - 1) + (2\tilde{h}_L - 1)\sqrt{1 - (2\tilde{h}_L - 1)^2}] \tag{21}$$

$$\tilde{A}_G = 0.25\ [\cos^{-1}(2\tilde{h}_L - 1) - (2\tilde{h}_L - 1)\sqrt{1 - (2\tilde{h}_L - 1)^2}] \tag{22}$$

$$\tilde{S}_L = \pi - \cos^{-1}(2\tilde{h}_L - 1) \tag{23}$$

$$\tilde{S}_G = \cos^{-1}(2\tilde{h}_L - 1) \tag{24}$$

$$\tilde{S}_i = \sqrt{1 - (2\tilde{h}_L - 1)^2} \tag{25}$$

$$\tilde{U}_L = \tilde{A}/\tilde{A}_L \tag{26}$$

$$\tilde{U}_G = \tilde{A}/\tilde{A}_G \tag{27}$$

Both $X^2$ and Y can be calculated directly from a knowledge of pipe diameter, flow rates and fluid properties. Z, however, requires a knowledge of the liquid level in order to obtain $f_e$. Since, in this application the electric field is perpendicular to the pipe, $\gamma = 90^o$ and Z is set to zero. Similarly, as the pipe is horizontal, Y is also set equal to zero. Horizontal flow and a perpendicular electric field will be assumed throughout the rest of the paper. With these assumptions, $h_L$ can be unambiguously calculated with a knowledge of the flow rates alone.

## 2.3 Flow Regime Transition Criteria

### 2.3.1 Transition From the Stratified to the Intermittent or Annular Flow Regimes

The intermittent flow regime covers the plug (elongated bubble), slug and wavy annular regimes. Flow in these regimes starts as stratified flow. As the liquid flow rate is increased, the waves will tend to reach the top of the pipe forming a bridge. For plug and slug flow a complete bridge is formed. For annular flow there is not enough water to completely fill the pipe so the water is swept up and around the walls of the pipe.

First consider a wave existing on the surface of a stratified flow (Figure 2.3.1.1). As the gas passes over the wave, its speed increases due to the decreased area. This creates a lower pressure at the crest which will tend to make the wave grow. On the other hand, the difference in liquid levels makes the wave grow smaller. An unstable wave is created when the pressure forces are greater than the

gravitational forces. This causes the wave to grow. The force from an electric field also causes the wave to grow. For the moment the exact form of the electrical force (equations (9) and (10) will not be used, and it will be expressed in the general form $\Delta h\ f_e$, where $\Delta h$ is the height difference between the trough and crest of the wave, and $f_e$ is the remainder of either equation (9) or (10), depending on whether the water is considered as a dielectric or a conductor.

The criterion for wave growth is,

$$p - p' + \Delta h\ fe > (h_G - h'_G)\ (\rho_L - \rho_G)g \tag{28}$$

From the Bernouilli equation,

$$p - p' = 0.5\ \rho_G\ (U'^2_G - U^2_G) \tag{29}$$

Equating (28) and (29) and noting that the gas velocity is inversely proportional to the gas area gives,

$$U_G > \left[ \frac{2(h'_L - h_L)\ (\rho_L - \rho_G)g - f_e}{\rho_G} \quad \frac{A'^2_G}{A^2_G - A'^2_G} \right]^{0.5} \tag{30}$$

For small perturbations $A'_G$ can be expanded in a Taylor series about $A_G$,

$$A'_G = A_G - (h'_L - h_L)\ d\ A_L/dh_L \tag{31}$$

Substituting equation (31) into equation (30) gives,

$$U_G > C_2 \left[ \frac{[(\rho_L - \rho_G)g - f_e]' A_G}{dA_L/dh_L} \right]^{0.5} \tag{32}$$

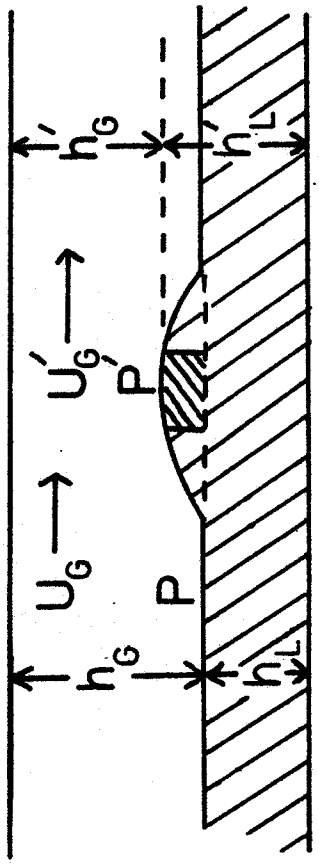


FIGURE 2.3.1.1: INSTABILITY FOR A SOLITARY WAVE

where $C_2 = A'_G/A_G$. The value of $C_2$ is not known, however Taitel and Dukler, 1976, found that $C_2 = 1 - h_L/D$ gave results consistent with those of Kordyban and Ranov, 1973, and Wallis and Dobson, 1973. In dimensionless form, equation (32) becomes,

$$F_e^2 \left[ \frac{1}{2} \cdot \frac{\tilde{V}_G \, d\tilde{A}_L/d\tilde{h}_L}{\tilde{A}_G} \right] \geq 1 \qquad (33)$$

where $F_e$ is an electric Froude number of the form,

$$F_e = \frac{U_G^S}{\sqrt{D}} \left[ \frac{\rho_G}{(\rho_L - \rho_G) g - f_e} \right]^{1/2} \qquad (34)$$

and $d\tilde{A}_L/d\tilde{h}_L$ can easily be found from the expression for $\tilde{A}_L$.

It should be noted that if the electric field goes to zero, then the expression reduces to the formula obtained by Taitel and Dukler, 1976. Note also that the exact liquid composition has not been defined yet. It could be either a dielectric or a conductor, depending on the expressions used.

From the electric Froude number it can be seen that the electric field acts as a destabilizing influence, causing the transition to occur at lower flow rates than without it.

### 2.3.2 Transition from Intermittent to Annular Flow

As noted in section 2.3.1, the same phenomenon that causes slug flow, also causes annular flow. The only difference between the two flows is that there is not enough water to completely fill the pipe in annular flow. This suggests that the occurence of a slug or annular flow depends on the liquid level in the pipe. As a result, annular

flow is assumed to occur at liquid levels below 0.5 $h_L$, and slug flow occurs at liquid levels above this value (Taitel and Dukler, 1976), providing the transition criterion for intermittent flow is met.

The analysis in section 2.3.1 shows that the electric field will not affect the fluid level. Therefore it will not have an effect on this transition.

### 2.3.3 Transition from Stratified Smooth to Stratified Wavy Flow

Stratified wavy flow occurs when the gas velocity is great enough to cause waves, but lower than that needed to cause the rapid wave growth characteristic of intermittent or annular flow. This happens when the force of the wind is great enough to overcome the viscous dissipation of the wave.

According to Lamb, 1945, the viscous dissipation of energy per unit time of a wave can be expressed as $2\mu k^3 c^2 \alpha^2$, where $\mu$ is the viscosity, k is the wave number, c is the phase velocity and $\alpha$ is the amplitude. The air pressure acting on the surface of the wave only makes a positive contribution if it is acting in phase and at the same frequency as the wave. It is postulated that the pressure due to the wind can be broken up into Fourier components, one of which has the frequency of the wave, $\omega$.

$$\Delta p_\omega = C \cos (\omega t - kx) \tag{35}$$

where C is a constant, and $\Delta p$ is the variation in pressure due to the wind. C has been evaluated as $C = \beta \rho_G (U_G - C)^2 k\alpha$ (Jeffreys, 1929).

$\rho_G$ is the gas density, $U_G$ is the gas velocity, and the other variables are defined as before. $\beta$ is what Jeffreys called a sheltering coefficient. Jeffreys estimated this value to be 0.3, but Taitel and Dukler, 1976, used a value of 0.01 based on more accurate data.

Due to the nature of the electric force, it always acts in phase with the wave, and against the viscous force. This can be expressed as,

$$\Delta p_e = B\cos(\omega t - kx) \tag{36}$$

From the arguments in section 2.3.1, $B = 2\alpha f_e$. Both the electric force and wind pressure are added to the viscous dissipation to account for the change in internal energy of the wave.

$$\frac{d}{dt}\left(1/2(\rho_L - \rho_G)kc^2\alpha^2\right) = \frac{1}{2}kc\alpha C + \frac{1}{2}kc\alpha B - 2\mu k^3c^2\alpha^2 \tag{37}$$

After differentiating and rearranging we obtain,

$$\frac{d\alpha}{dt} = \frac{C}{2(\rho_L - \rho_G)c} + \frac{B}{2(\rho_L - \rho_G)c} - 2\nu k^2\alpha \tag{38}$$

where $\nu$ is the kinematic viscosity of the fluid.

In order for the wave not to dissipate due to viscous forces, the right hand side of equation (38) must be greater than or equal to zero. Upon rearrangement and substitution for C and B, the following expression is obtained,

$$(U_G - c) \geq \frac{4\nu k^2(\rho_L - \rho_G)c - 2f_e}{\beta\rho_G k} \tag{39}$$

In order to put this into a more workable form, three assumptions must be made (Lamb, 1945). The first is that capillarity can be neglected. This give $c^2 = g/k$. The second assumption is that $U_g >> c$. The third assumption is based on the premise that the ratio of wave velocity to film velocity decreases with increasing Reynolds number. For turbulent flow this ratio is approximately equal to 1, so c is set equal to $U_L$ for simplicity. Using these approximations gives,

$$U_G > \left[ \frac{4\nu(\rho_L - \rho_G)g^2 - 2f_e U_L^3}{\beta \rho_G U_L} \right]^{\frac{1}{2}} \tag{40}$$

It should be noted here that $\nu$ is the viscosity of the liquid, not the gas. Equation (40) can be expressed in terms of known and dimensionless quantities,

$$\tilde{U}_G > \left[ \frac{4\nu(\rho_L - \rho_G)g^2 - 2f_e \tilde{U}_L^3 \, (U_L^S)^3}{\beta \rho_G \tilde{U}_L (U_L^S)(U_G^S)^2} \right]^{\frac{1}{2}} \tag{41}$$

### 2.3.4 Transition from Intermittent to Dispersed Bubble Flow

The transition to dispersed bubble flow occurs when the force on the gas bubbles due to turbulent fluctuations in the liquid flow are great enough to overcome the buoyant force of the bubble (Taitel and Dukler, 1976). The buoyant force per unit length on the gas is

$$F_B = g(\rho_L - \rho_G)A_G \tag{42}$$

The force acting due to turbulence is estimated in a manner used by Levich, 1962.

$$F_T = \frac{1}{2} \rho_L \overline{v'^2} \, S_i \tag{43}$$

where v' is the radial velocity fluctuation whose root-mean-square is estimated to be approximately equal to the frictional velocity,

$$\left(\overline{v'^2}\right)^{\frac{1}{2}} = U_L\left(\frac{f_L}{2}\right)^{\frac{1}{2}} \tag{44}$$

The electric field acts as an upward force on the bottom of the bubble while the bubble is in contact with the upper surface of the pipe. The force per unit length is given by equation 1 or 2, depending on whether the fluid is considered a dielectric or conductor, multiplied by the gas-liquid interfacial perimeter, $S_i$. Similar to the approach previously taken, the electric force will be represented by a constant, $P_E$. It should be noted that $P_E$ is not the same as $f_e$ used previously; $f_e$ was taken from equation 9 or equation 10. This gives the force per unit length on the gas due to the electric field as,

$$F_E = P_E\, S_i \tag{45}$$

In order for bubble flow to occur, the turbulent force must be great enough to overcome the buoyant and electric forces on the bubble forcing it up against the top of the pipe. Mathematically this is expressed as,

$$\frac{1}{2}\rho_L U_L^2 \frac{f_L}{2} S_i \geq g(\rho_L - \rho_G)A_G + P_E\, S_i \tag{46}$$

Using dimensionless variables this becomes,

$$\tilde{U}_L \geq \frac{2(\tilde{D}_L\, \tilde{U}_L D U_L^S/\nu_L)^{-n/2}}{\sqrt{C_L\, \rho_L\, U_L^S}} \left[\frac{g(\rho_L - \rho_G)\tilde{A}_G D + P_E}{\tilde{S}_i}\right]^{\frac{1}{2}} \tag{47}$$

## 2.4 Numerical Procedures

The three equations that need to be solved are equations (33), (41) and (47). All three each have to be solved in conjunction with equation (17). All values can be determined except $U_L^S$, $U_G^S$ and $h_L$ (all dimensionless variables can be expressed in terms of $h_L$).

The solutions were found using the dielectric model of water. The only difference in the equations for the dielectric and conducting water model is the factor of $(1 - \varepsilon^{(2)}/\varepsilon^{(1)})$ in the equation for electric force. Since $\varepsilon^{(1)}$ is approximately 72(water at 25°C) and $\varepsilon^{(2)}$ is approximately 1.0 (air at the same temperature), this factor is extremely close to 1 and will affect the answer only slightly.

The easiest method of solution found was to fix $h_L$, then use the two equations to solve for $U_L^S$ and $U_G^S$. The flow charts for the transition calculations are shown in Figures 2.4.1 to 2.4.3. Notice that the transition from slug to annular flow is not calculated. This is because only the liquid level is necessary to calculate the transition. Also note that the electric force is dependent on the liquid level and can easily be found if this is known. The computer programs are listed in Appendix 1.

## 2.5 Theoretical Results

The numerical results for the stratified smooth to slug transition using equations (17) and (33) to predict the flow transition under an electric field for a 0.019 m. and 0.0127 m. internal diameter pipe are shown in Figures 2.5.1 and 2.5.2 respectively. It should be noted that the result without applied voltage is equivalent to the

results obtained by Taitel and Dukler, 1976. The applied voltage causes the transition from stratified to slug flow to occur at lower air and water flows. The effect increases as the voltage is increased, being more pronounced at low air flows. This occurs because at low air flows the liquid level is near the top electrode, thus giving a large electric force.

The numerical results for the slug to dispersed bubbly flow transition is shown in Figures 2.5.3 and 2.5.4 for various applied voltages for internal pipe diameters of 0.019 m. and 0.0127 m. respectively.

The effect of applied voltage to this transition is the opposite to the transition from stratified to slug flow. This is to be expected as the electric force presses the bubble up against the top of the pipe, preventing it from mixing with the liquid. The same pattern as in the stratified to intermittent transition of the effect becoming more pronounced at low gas flows is followed for the same reason as before. The force due to the electric field is larger for higher liquid levels.

Only the zero voltage results for the transition from stratified smooth to stratified wavy is shown in Figure 2.5.5 for the 0.019 m. and the 0.0127 m. internal diameter pipes. This is because the transition occurred at extremely low air and water flows for the voltages used in the calculations.

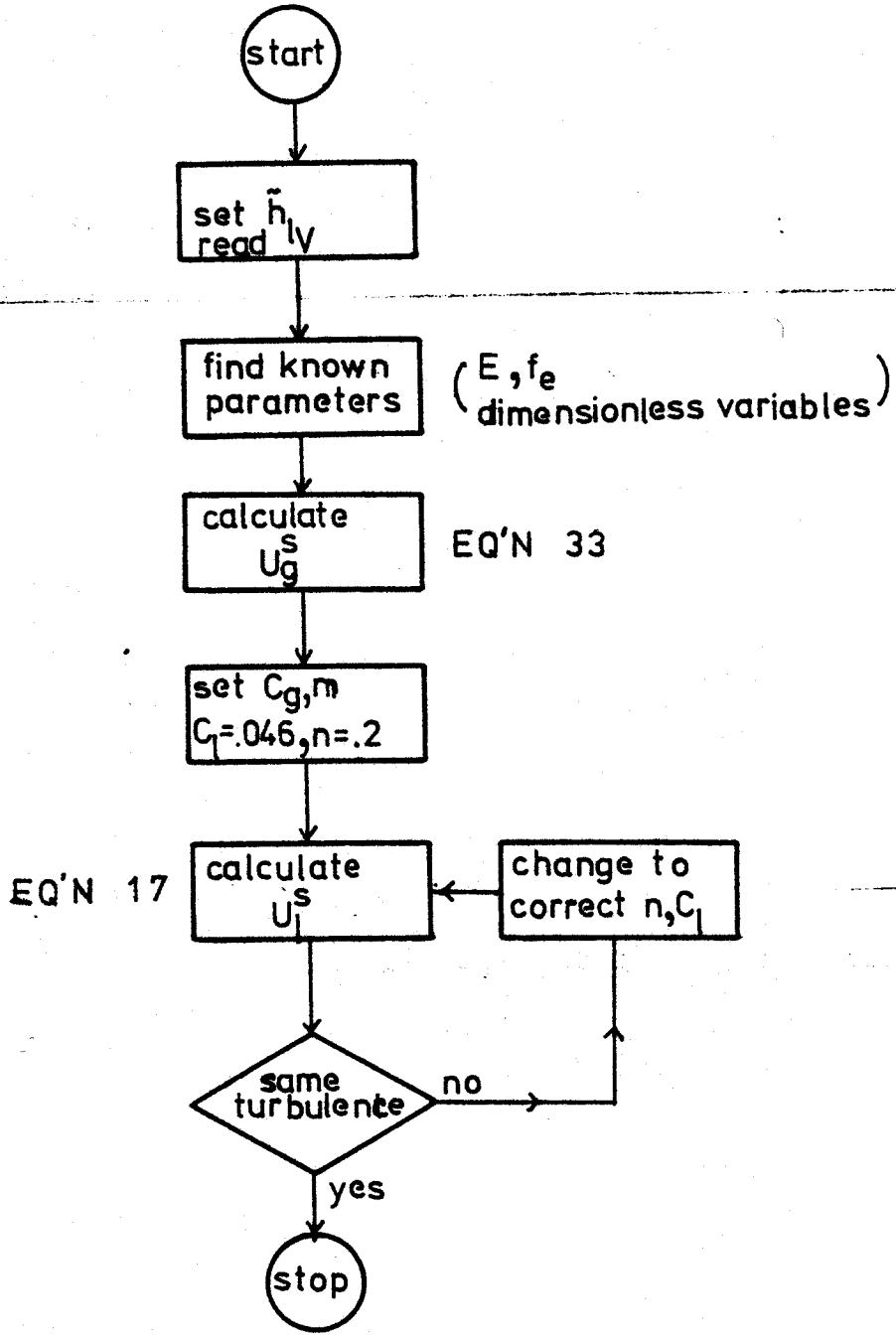


FIGURE 2.4.1: STRATIFIED TO INTERMITTENT TRANSITION

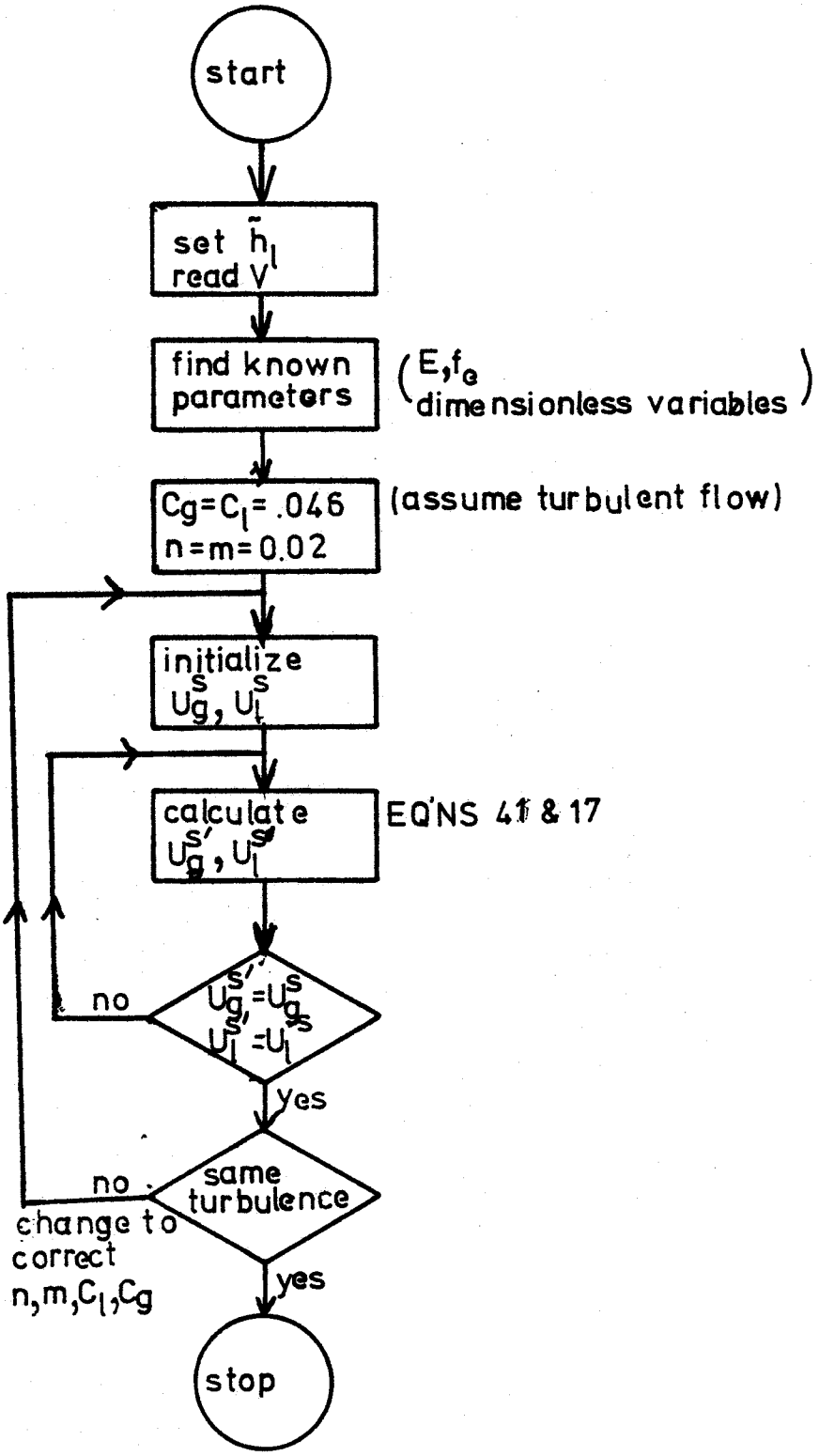


FIGURE 2.4.2: STRATIFIED SMOOTH TO STRATIFIED WAVY TRANSITION

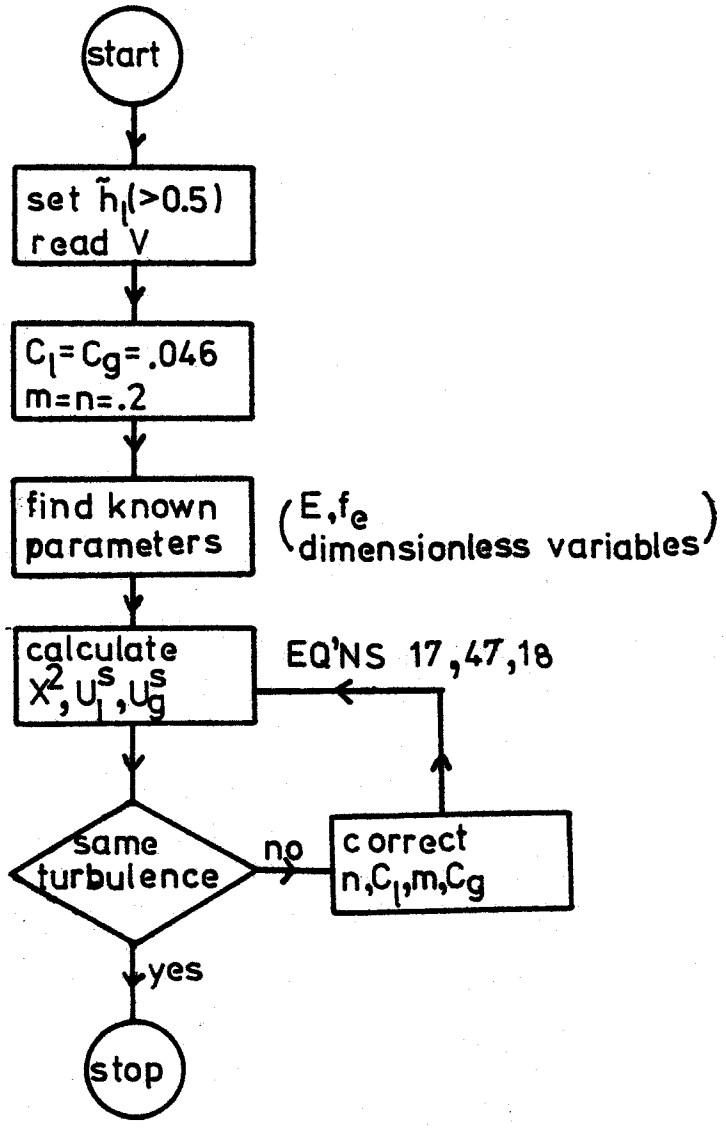


FIGURE 2.4.3: INTERMITTENT TO BUBBLY TRANSITION

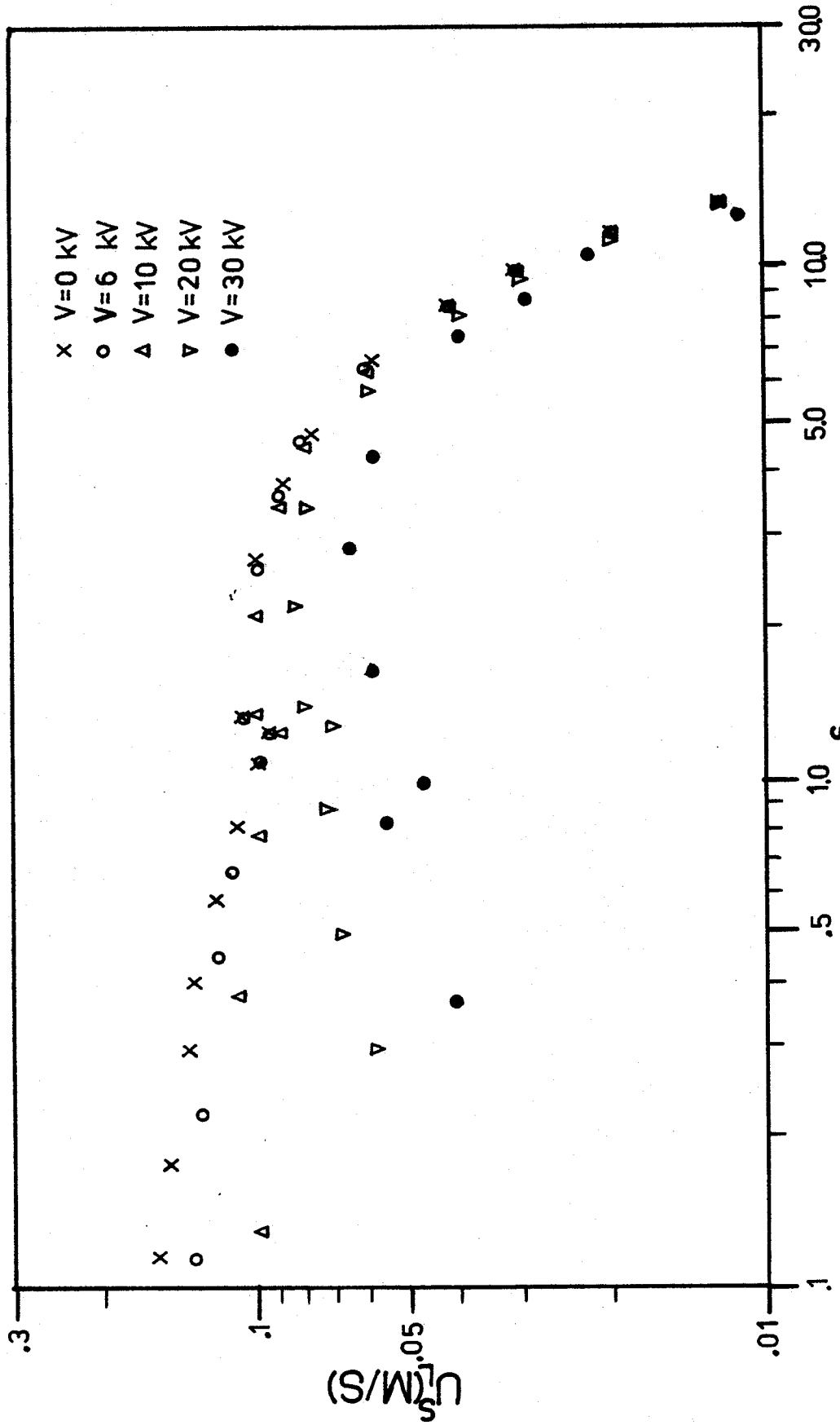


FIGURE 2.5.1: PREDICTED STRATIFIED–INTERMITTENT TRANSITION FOR A .019 m INTERNAL DIAMETER HORIZONTAL PIPE

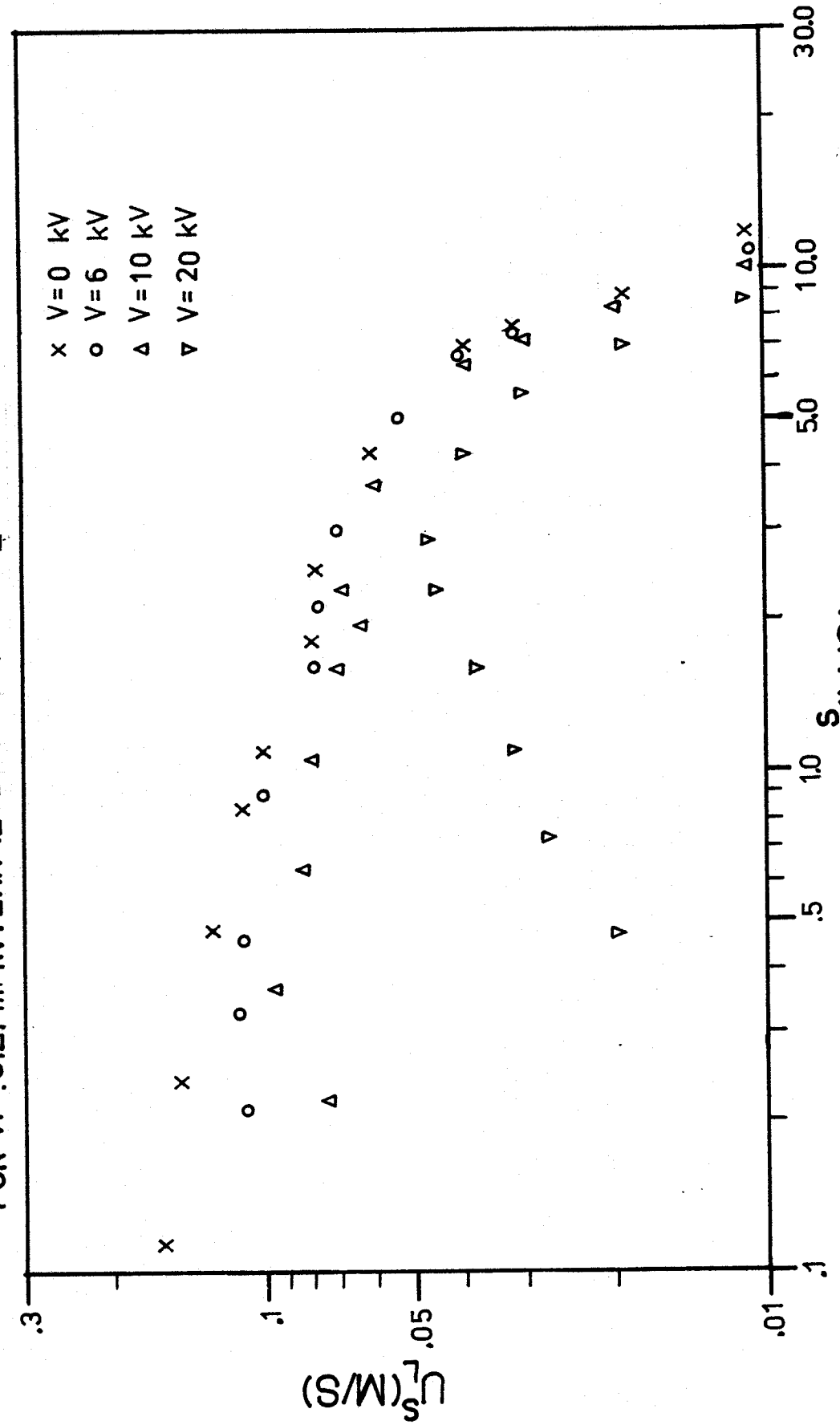


FIGURE 2.5.2: PREDICTED STRATIFIED-INTERMITTENT TRANSITION FOR A .0127 m. INTERNAL DIAMETER HORIZONTAL PIPE

FIGURE 2.5.4: PREDICTED INTERMITTENT-BUBBLY TRANSITION FOR A .0127 m. INTERNAL DIAMETER HORIZONTAL PIPE

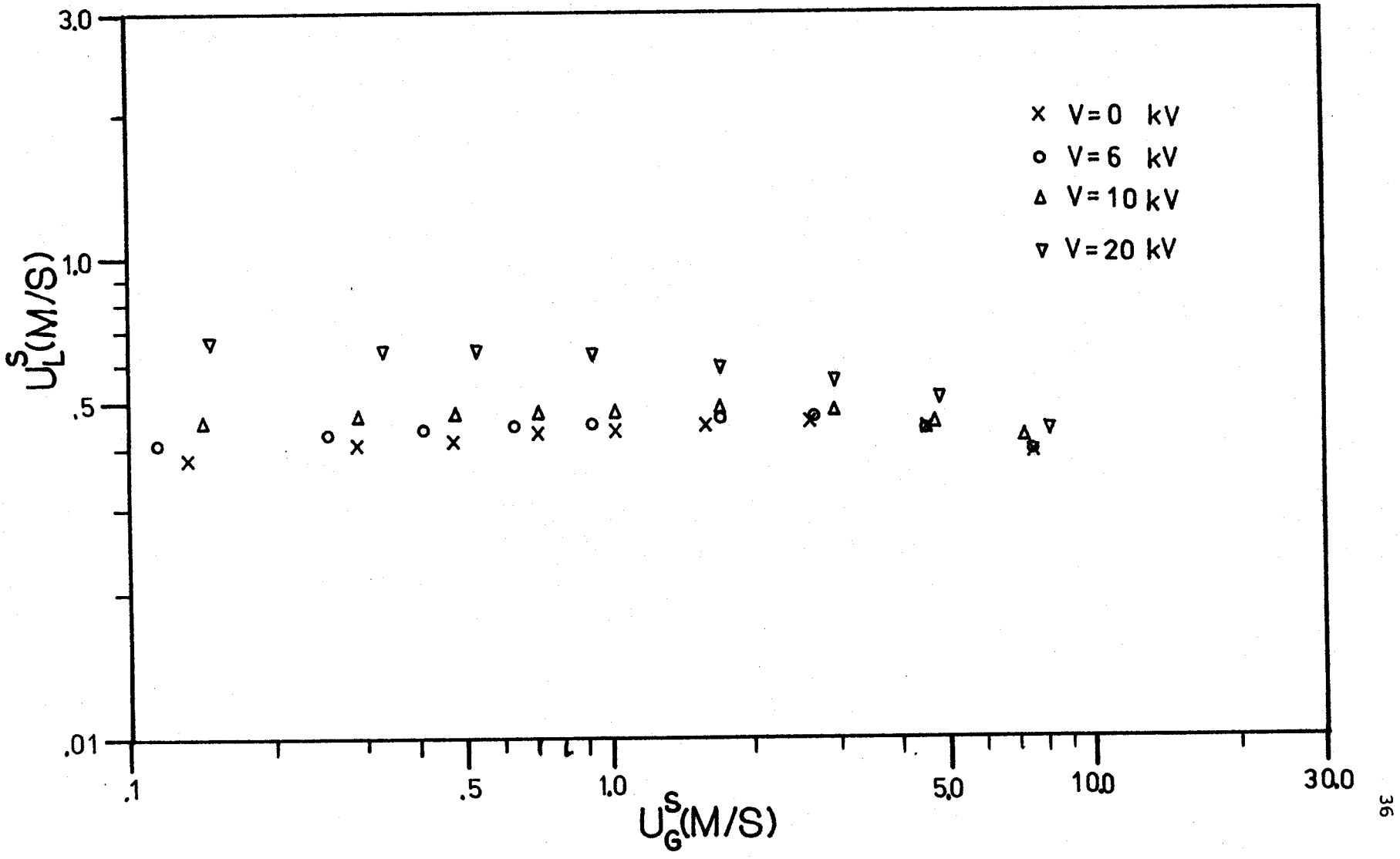

FIGURE 2.5.3: PREDICTED INTERMITTENT–BUBBLY TRANSITION FOR A .019 m. INTERNAL DIAMETER HORIZONTAL PIPE

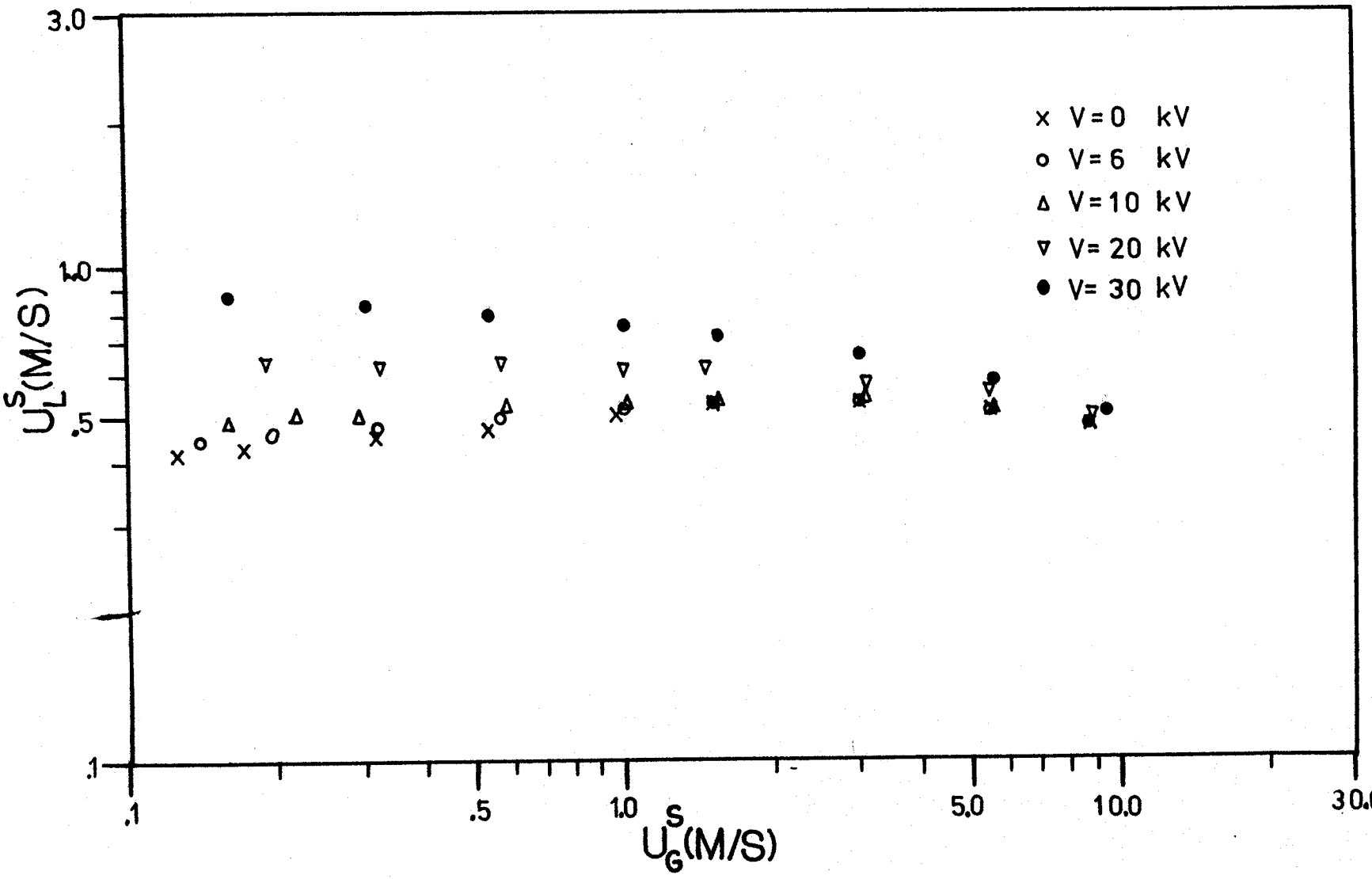

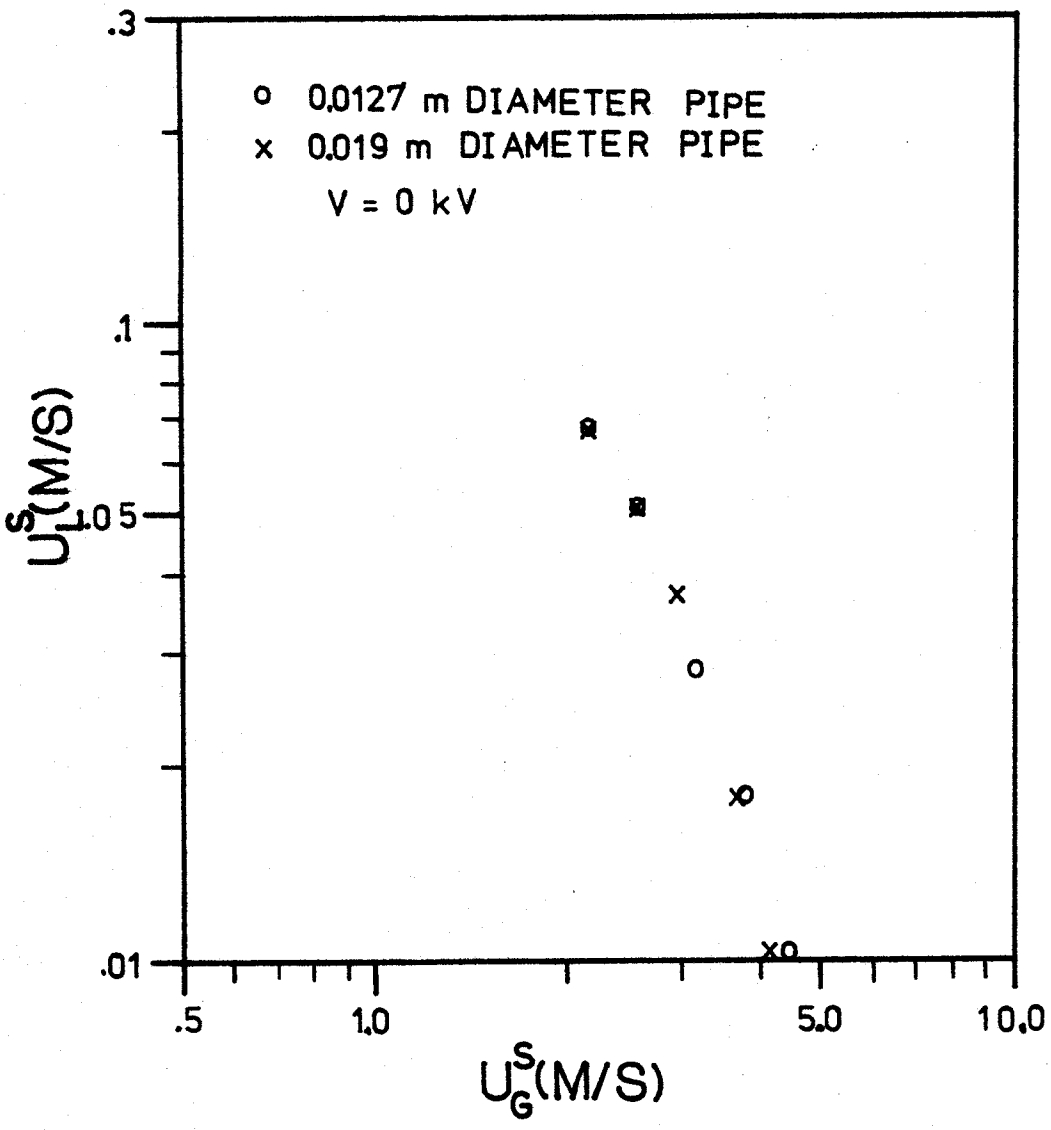


FIGURE 2.5.5: STRATIFIED SMOOTH TO STRATIFIED WAVY TRANSITION IN 0.0127 AND 0.019 m INTERNAL DIAMETER HORIZONTAL PIPES

CHAPTER 3

# Experimental Method

## 3.1 Experimental Apparatus

A schematic of the experimental equipment is shown in Figure 3.1.1. Compressed air was taken from the laboratory supply and filtered before being injected into the pipe. The water supply was tap water from the city supply.

Two different internal diameter acrylic pipes were used, one of internal diameter 1.27 cm. (1/2") and the other of internal diameter 1.9 cm. (3/4"), both with a .32 cm (1/8") wall thickness. The air-water inlet was through a t-junction, the water being injected from the bottom and the air from the rear.

The 1.27 cm. pipe was about 10 feet long while the 1.9 cm. pipe was 6 feet long. Both emptied into an open container so as to offer as little interference as possible with the water flow. The 1.27 cm. pipe consisted of two joined lengths of pipe. As the join appeared to cause interference with the flow, only slugs, waves, etc. which appeared before the join were considered as genuine. As the join was 6 feet from the inlet the flow is fully developed by this time.

The electrodes were two flat pieces of aluminum 12 inches long, 3 inches wide and rounded at the edges to reduce corona effects. The

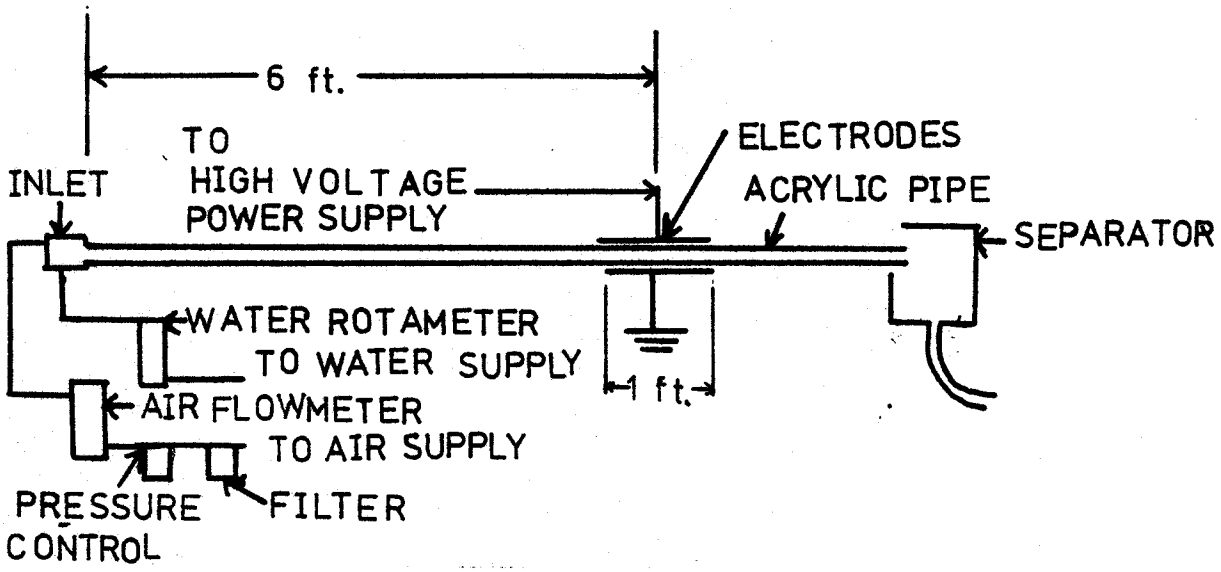


FIGURE 3.0.1: SCHEMATIC OF EXPERIMENTAL APPARATUS

bottom electrode was grounded and helped support the pipe. The top electrode had a negative charge and was not put into contact with the pipe to reduce the possibility of electrical leakage along the surface of the pipe. However it was close enough so that the outside diameter of the pipe could be taken as the distance between the electrodes.

Two rotameters were used to measure the air flow, one of capacity 5 l/min., and the other 30 l/min. A similar arrangement was used for water flow, the rotameters being of 2 l/min. and 5 l/min. capacity.

A 100 KV D.C. Universal Voltronics power supply was used, although it was never used to this high a voltage due to corona discharges.

## 3.2 Procedure

The pipe was set horizontal using a spirit level. The experiments were then run at zero voltage in order to see how close the results came to theory at zero voltage, and to act as a reference for the change in flow transitions. Both water and air flow were varied logarithmically in order to get even coverage of the graph. Water flow ranged from .08 l/min. to 2.8 l/min. for the 1.27 cm. pipe, giving specific velocities from .01 $^{m}$/s to .37 $^{m}$/s. Air flow in the same pipe went from 3.5 l/min. to 30 l/min, giving specific velocities from .45 $^{m}$/s to 4.0 $^{m}$/s.

Water flow in the 1.9 cm. pipe ranges from .18 l/min. to 4.5 $^{\ell}$/m giving specific velocities from .01 $^{m}$/s to .27 $^{m}$/s. Air flow ranged from 5.0 $^{\ell}$/m to 30 $^{\ell}$/min. giving specific velocities from .29 $^{m}$/s to 1.75 $^{m}$/s.

Air flow velocities much higher than those achieved were needed in order to get a complete flow regime map. However, the laboratory air supply couldn't give enough pressure.

Two runs were made at each voltage, one with the air flow held constant while the liquid flow was varied and another with the liquid flow held constant while the air flow was varied. A combination of the two runs was used for the final flow regime map.

Flow regimes were determined visually. Although some regimes were easy to ascertain, such as the slug or elongated bubble regime, the difference between stratified and stratified wavy or slug and wavy annular were largely a matter of judgement. An attempt was made to be consistent by defining more rigidly what these flow regimes were. In order for flow to be consider wavy, a definite wave had to be seen travelling down the pipe. Surface motion alone was not enough.

For flow to be wavy annular, the wave must be either just barely touching the top of the pipe or very frothy. The transition from elongated bubble to slug flow is easily defined. Slug flow occurs when air bubbles are entrained in the liquid bridge.

After the zero voltage map was established, the voltage was increased until just before breakdown started to occur. This was 20 kV in the case of the 1.27 cm. pipe, and 30 kV for the 1.9 cm. pipe. A certain amount of holding of the charge was observed to occur when the voltage was turned down. This did not disappear for a couple of hours after. As a result the measurements were always taken in order of ascending voltage.

CHAPTER 4

# Experimental Results and Discussion

## 4.1 Experimental Results

The maps of the observed flow regimes are given in Figures 4.1.1 to 4.1.6. The flow regimes are represented by the symbols as defined in Table 4.1.1.

The three transitions which are applicable over the range of flow rates examined are the stratified-intermittent, the stratified smooth-stratified wavy and the intermittent-annular transitions. These are shown in Figures 4.1.1 to 4.1.6 by the solid line.

The stratified smooth-stratified wavy transition is only shown for the zero voltage case as theoretical predictions indicated wavy flow for the flow rates used when an electric field is applied. As no prediction for the plug to slug transition is made, the two regions are differentiated just for interest.

## 4.2 Discussion

The flow regime map without an applied electric field is shown in Figures 4.1.1 and 4.1.4 for the 0.0127 m. and the 0.019 m. internal diameter pipes respectively. The results for both pipes shows fairly good agreement with theory except for the stratified smooth ~~to stratified smooth~~ to stratified wavy transition. This takes place at much

# TABLE 4.1.1

## SYMBOLS USED TO IDENTIFY DIFFERENT FLOW REGIMES

| | |
|---|---|
| Δ | STRATIFIED SMOOTH |
| x | STRATIFIED WAVY |
| o | PLUG |
| ▽ | SLUG |
| ● | WAVY ANNULAR |
| —— | TRANSITIONS USING PRESENT MODEL |

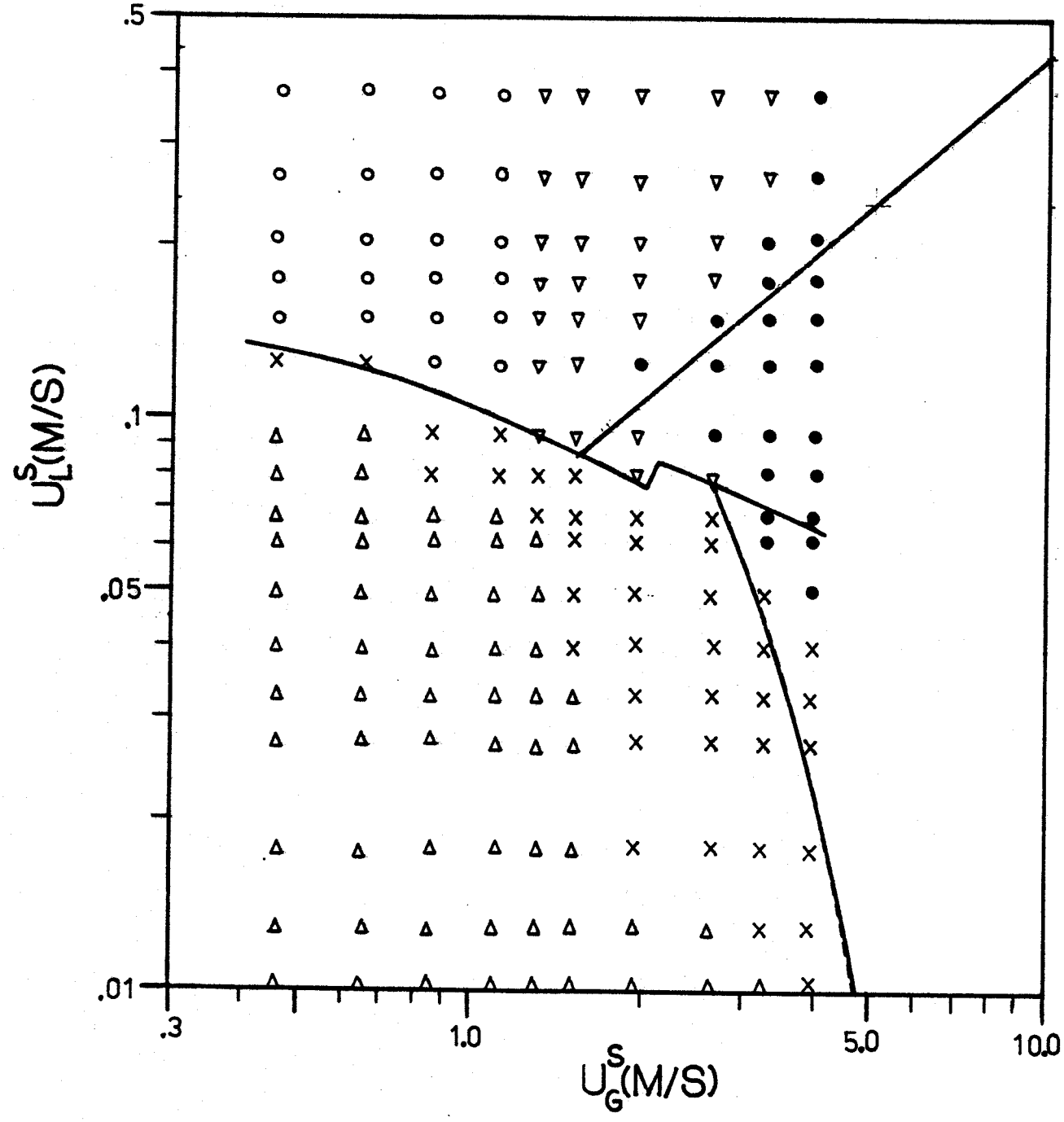


FIGURE 4.11: FLOW REGIMES OBSERVED IN A PIPE .0127 m. INTERNAL DIAMETER AND V=0 kV

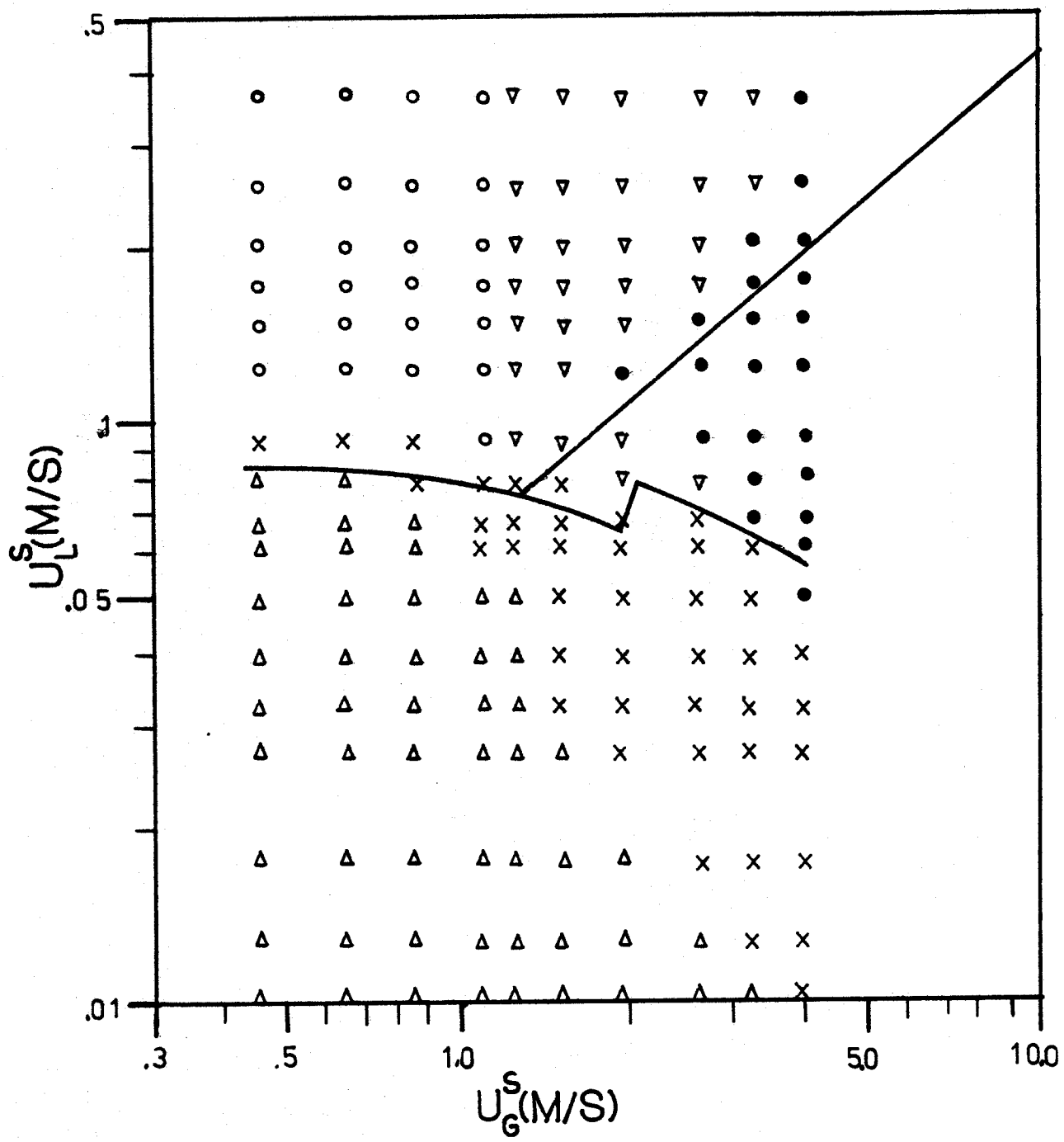


FIGURE 4.1.2 : FLOW REGIMES OBSERVED IN A PIPE .0127 m. INTERNAL DIAMETER AND V=10kV

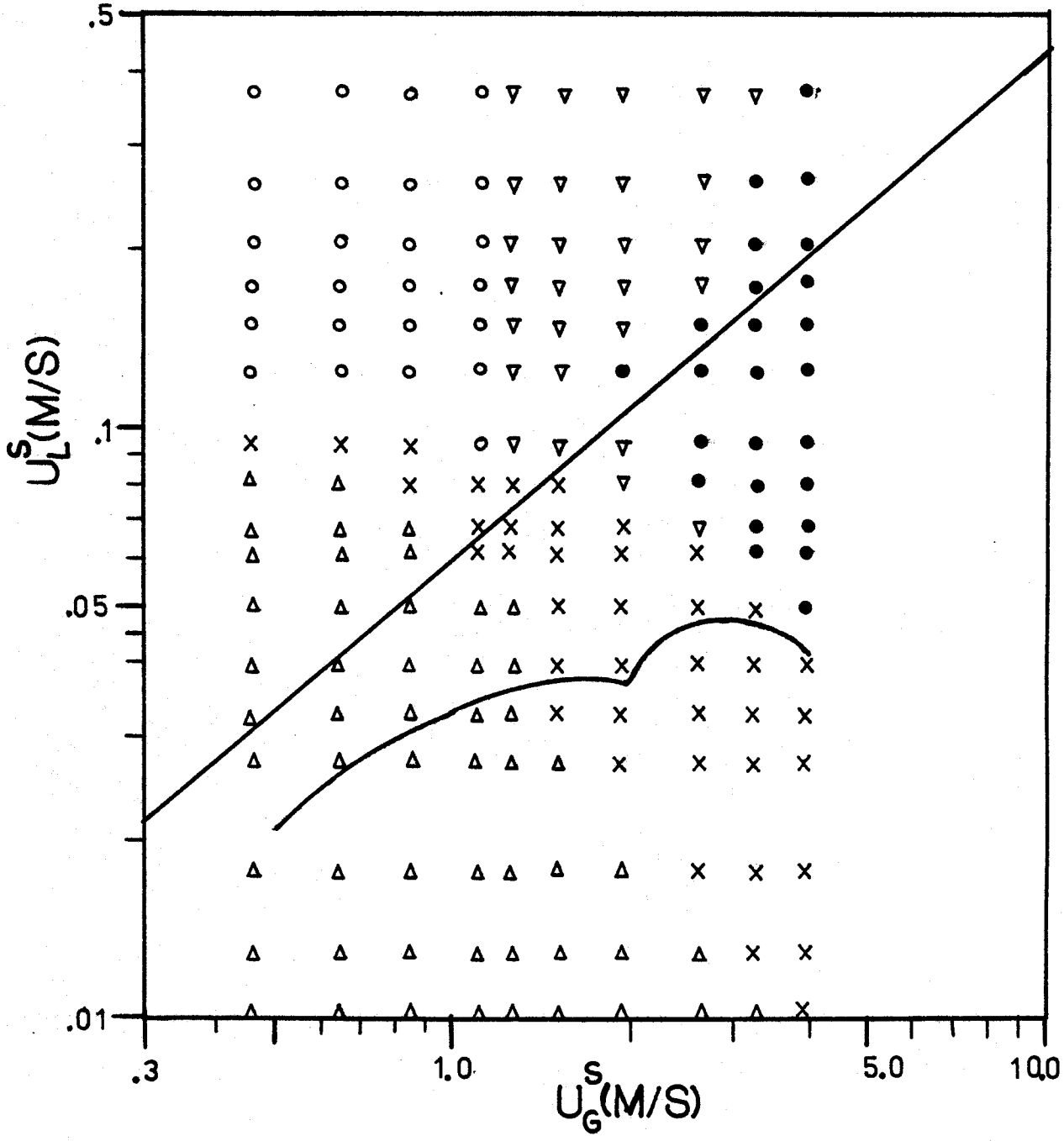


FIGURE 4.1.3: FLOW REGIMES OBSERVED IN A PIPE .0127 m. INTERNAL DIAMETER AND V=20 kV

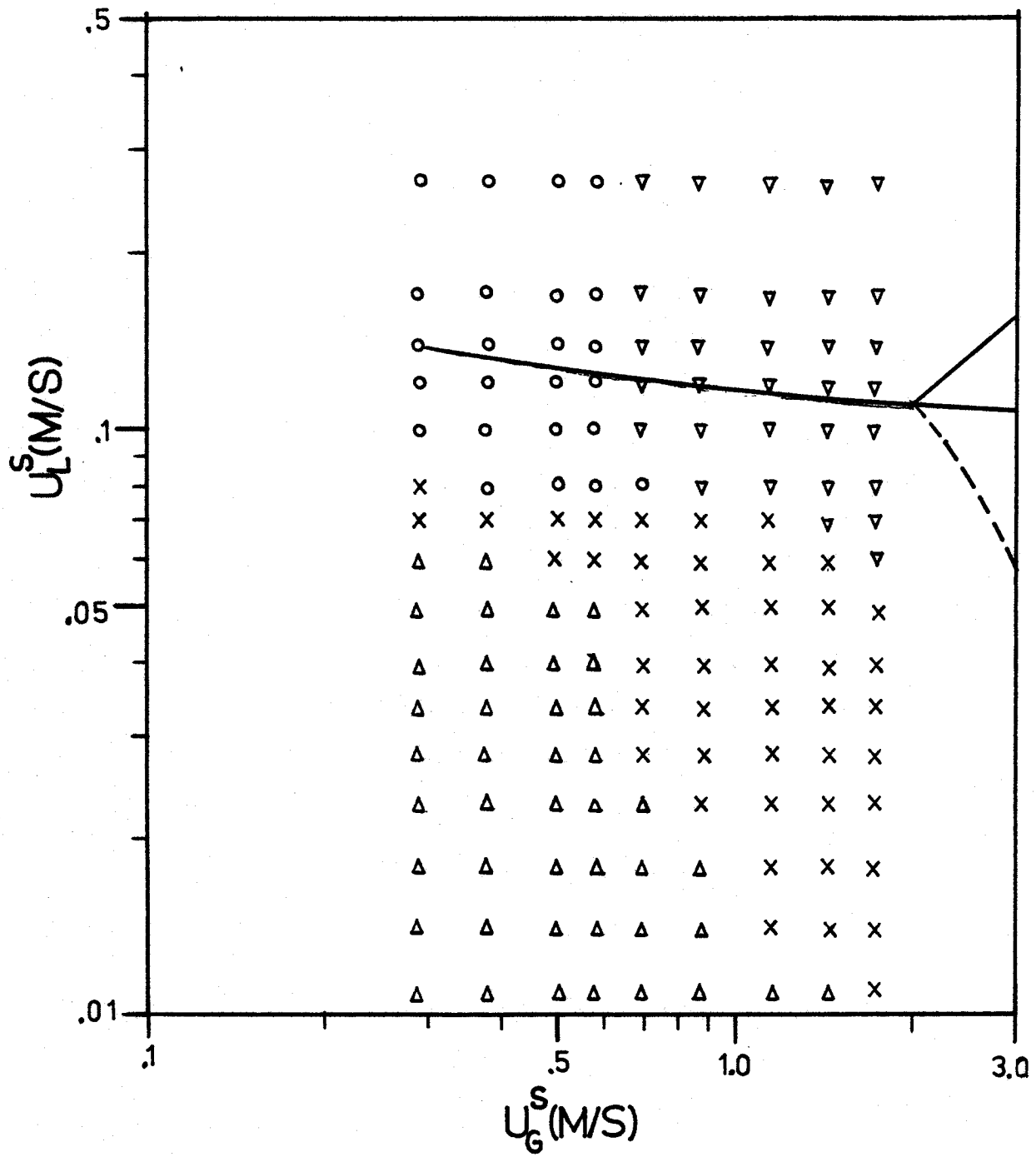


FIGURE 4.1.4: FLOW REGIMES OBSERVED IN A PIPE .019 m. INTERNAL DIAMETER AND V=0 kV

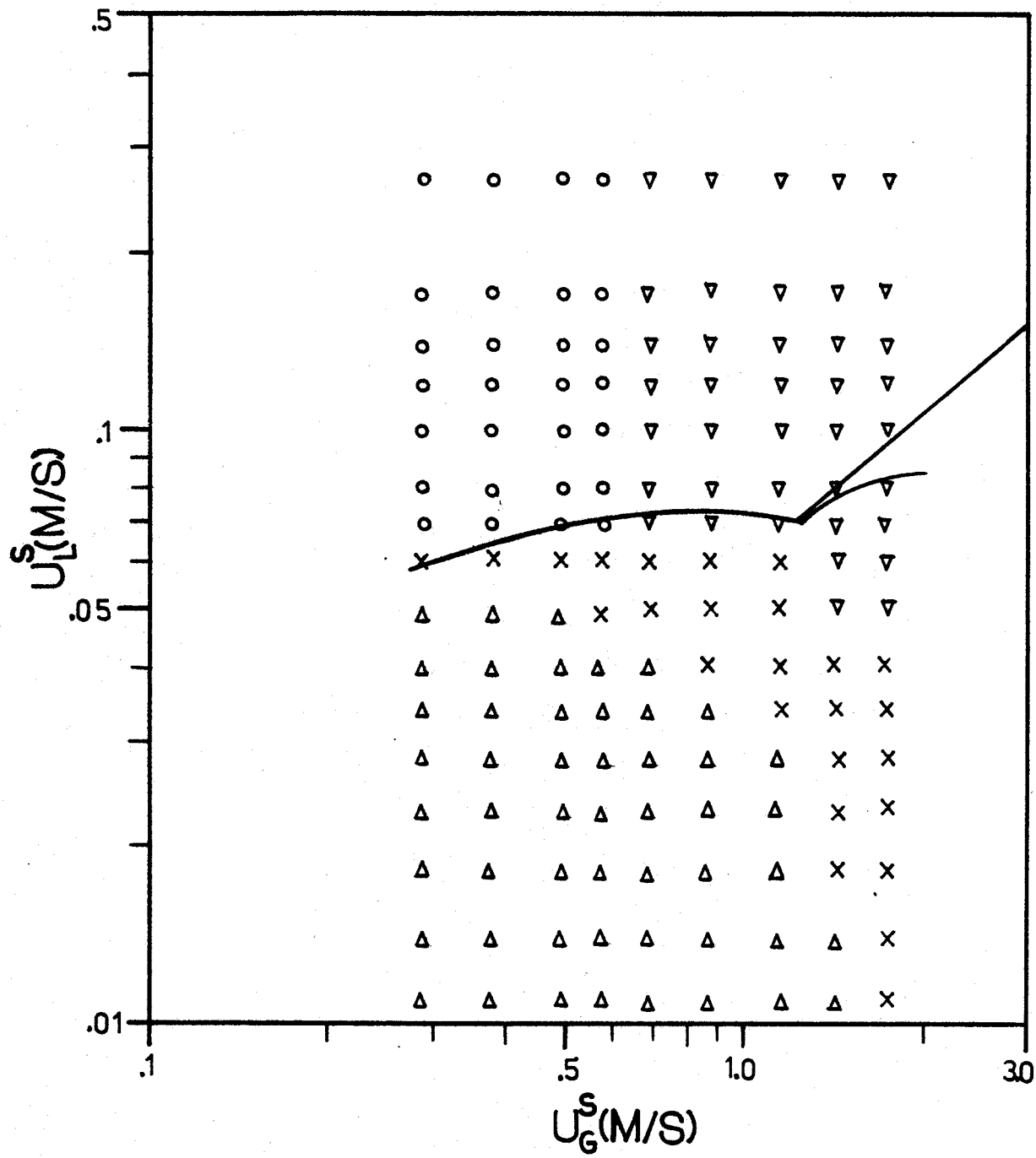


FIGURE 4.1.5: FLOW REGIMES OBSERVED IN A PIPE .019 m. INTERNAL DIAMETER AND V=20 kV

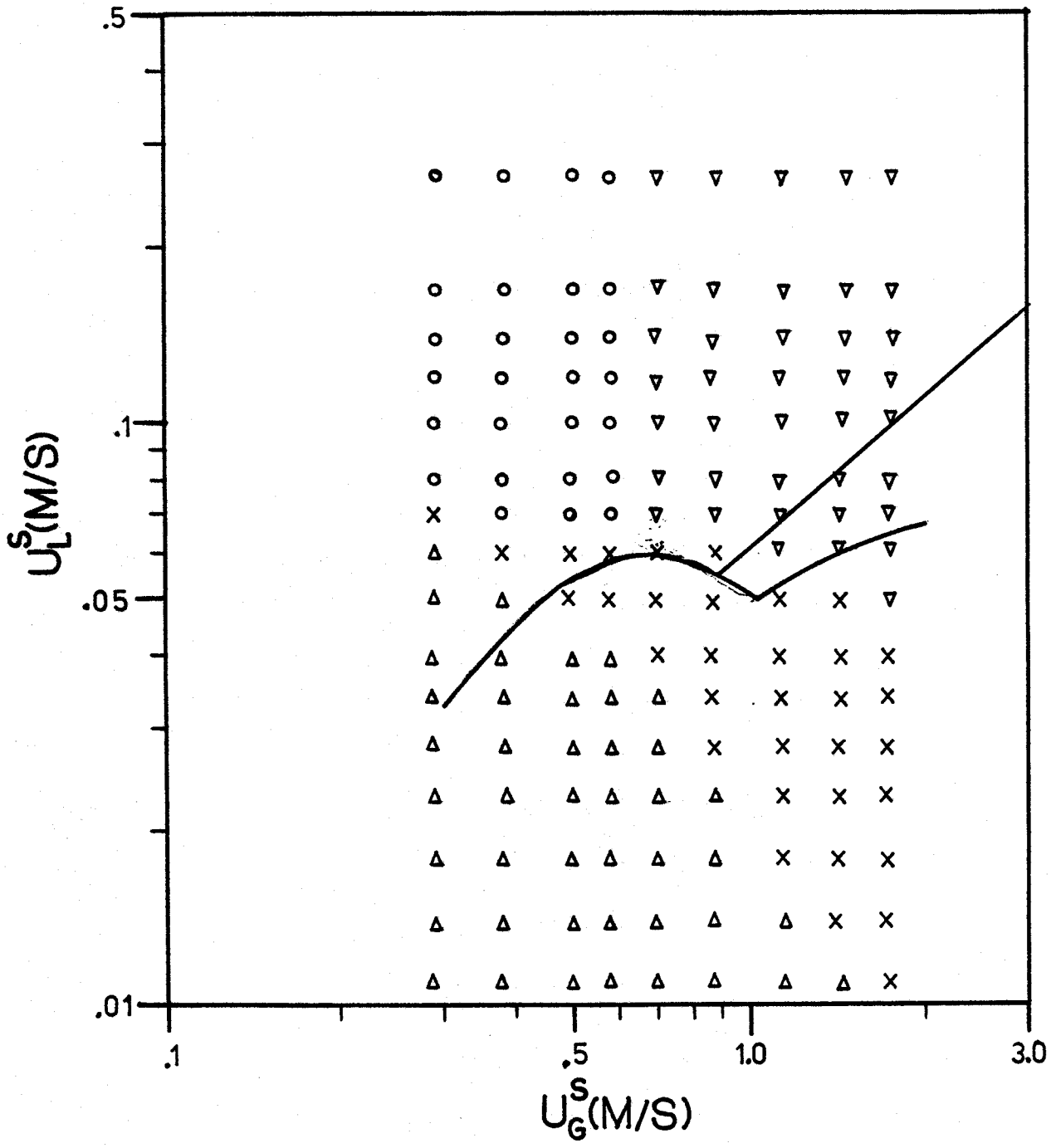


FIGURE 4.1.6: FLOW REGIMES OBSERVED IN A PIPE .019 m. INTERNAL DIAMETER AND V=30 kV

lower air flows than expected. This may be due to the following reasons: (1) entrance effects, although it would be expected that these would influence the other transitions as well; (2) the pipe has a slight upward tilt or bend causing the onset of slugging much earlier than would the case in an absolutely horizontal channel (Kordyban and Ranov, 1973); (3) the constitutive equations used in the numerical model may be inadequate to predict this transition; (4) the definition of the transition point to wavy flow is extremely subject to interpretation and may cause wide scatter in results.

Both flow regime maps show the standard flow regime pattern. Since the differences in the transitions due to the electric field are desired, comparison was made with respect to the maps at zero voltage. This eliminated any differences which could be caused by imperfections in the equipment.

The flow regime maps for the 0.0127 m. internal diameter pipe under applied voltages of 10 and 20 kV are shown in Figures 4.1.2 and 4.1.3 respectively, while the flow regime maps for the 0.019 m. internal diameter pipe under applied voltages of 20 and 30 kV are shown in Figures 4.1.5 and 4.1.6.

A comparison of the observed transitions at different voltages for the 0.0127 m. and the 0.019 m. internal diameter pipes are shown in Figures 4.2.1 and 4.2.2 respectively. The most notable thing observed when the electric field was applied was that there was very little effect on the flow regime transitions. There appears to be some slight destabilizing effect, but this is far less than predicted by the present theory.

A number of factors may account for this discrepancy. One is that the theory may be inadequate. A number of researchers (Choe, 1978, Kordyban, 1977, Weisman, 1979, Gardner, 1979) have questioned the validity of Taitel and Dukler's model. Choe, 1978, in particular notes that when the system is not an air-water system, Taitel and Dukler's results vary significantly from experimental results. This indicates that Taitel and Dukler's theory may not take fluid properties adequately into account. However, it is felt that their model is at least qualitatively adequate and should be able to predict the direction of the trend, which it does (see Figures 4.2.1 and 4.2.2).

A possible reason that such trends were not strongly indicated in the present experiment is because of the build-up of space-charge on the pipe. This would lessen the electric field felt by the surface of the water so that the effective electric field is much less than the applied electric field. Evidence supporting this contention is that when the voltage was turned down, a pattern of waves of much higher than normal amplitude appeared on the surface of the water between the electrodes. This phenomena may be due to the electric field caused by the space-charge. Of note concerning these waves is that they were stationary, even though, the air-water mixture was flowing in the pipe at the same time.

## 4.3 Future Research

The problem with the line of research taken in this study was that it was an all-or-nothing effort. Either the effect of the electric field on the flow regime was seen or, as happened to be the case, it wasn't. However, the fact that the electric field does have

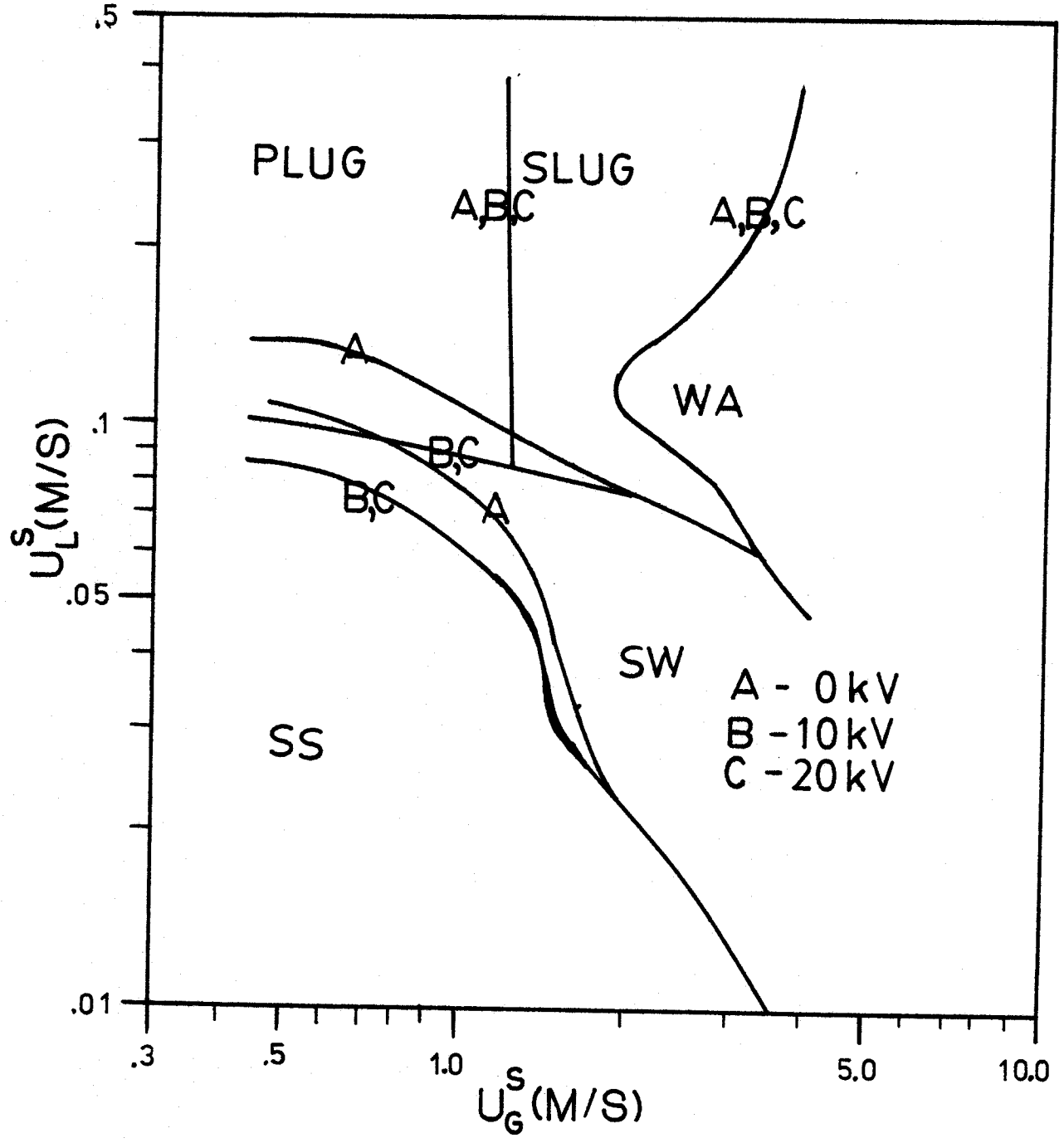


FIGURE 4.2.1: COMPARISON OF FLOW REGIMES OBSERVED IN A .0127 m. INTERNAL DIAMETER PIPE AT DIFFERENT VOLTAGES

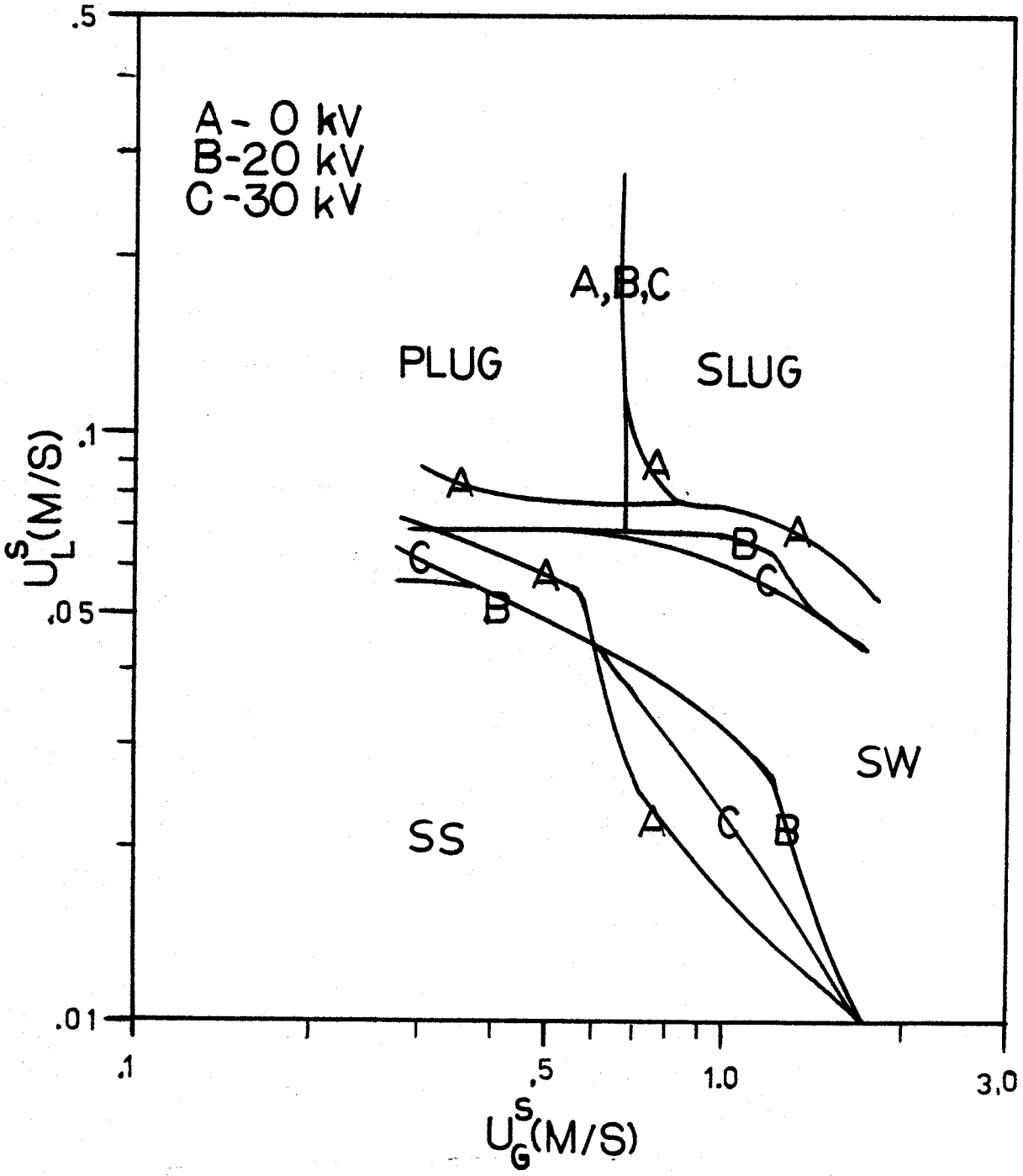


FIGURE 4.2.2: COMPARISON OF FLOW REGIMES OBSERVED IN A .019 m. INTERNAL DIAMETER PIPE AT DIFFERENT VOLTAGES

an effect on the flow is indisputable as evidenced by the appearance of stationary waves after the voltage is turned off. This single fact does not allow further insight into the mechanism or magnitude of the effect.

As a result the following lines of inquiry are proposed:

(1) Use a rectangular channel; such a geometry is much easier to handle mathematically, and permits much easier examination of theories of slug formation other than those of Taitel and Dukler.

(2) Measure the effect of the electric field on wave properties such as amplitude, wavelength and shape. Also, any effect on average liquid level should be noted. The best procedure is to use photographs because of the difficulty in using conductive probe measurements in a strong electric field. However, A.C. probe measurements may be possible.

(3) Perform the test with the test section and electrodes immersed in a dielectric. Hopefully this will stop the problem of buildup of charge on the electrodes. More over, a high voltage could be obtained before breakdown occurred.

(4) The effect of the electric field on a good conductor and a good dielectric should be tested. This would give insight as to whether the behaviour of the air-water interface is more typical of an insulator or a conductor.

Even though the above suggestions will not give the flow regime transitions, they will give enough information so that the correct form of the electric force can be used. This can then be put into existing theories and they can be tested for accuracy. Such a test will also reveal defects in the approach of the theories tested.

# CHAPTER 5

## Conclusion

The separated flow model was used to predict flow regime transitions for air-water flow in a horizontal pipe under the influence of an electric field applied perpendicular to the pipe. Numerical results predicted a destabilization of the stratified smooth to stratified wavy and the stratified to intermittent transition, while the intermittent to dispersed bubble transition was stabilized.

Observations were made on flow regimes in a 0.0127 m. and 0.019 m. internal diameter acrylic pipe. These showed good agreement at zero voltage, but did not show the change predicted by the model when voltage was applied, although the same trend was shown. This is thought to be due to the space-charge effect decreasing the effect of the electric field at the interface.

Suggestions for further experiments include detailed wave measurements in order to more accurately predict the magnitude of the electric force.

## BIBLIOGRAPHY


1. Agrawal, S.S., G.A. Gregory, and G.W. Govier, "An analysis of Horizontal Stratified Two-Phase Flow in Pipes", Canadian Journal of Chemical Engineering, 51, 280-286 (1973).

2. Aihara, Trans. Jap. Mech. Eng. Soc. 70, 583 (1967).

3. Ashmann, G., and R. Kronig, "The Influence of Electric Fields on the Convective Heat Transfer in Liquids", Appl. Sci. Res. A2, 235-244 (1951).

4. Baker, O., "Simultaneous Flow of Oil and Gas', Oil Gas J., 53 185 (July 1954).

5. Bonjour, E., Verdier, J., and Weil, L., "Electroconvection Effects on Heat Transfer", Chemical Engineering Progress, 58, 63-66, (1962).

6. Choe, W.G., Weinberg, L., and Weisman, J., "Observation and Correlation of Flow Pattern Transition in Horizontal, Co-current Gas-Liquid Flow", Two-Phase Transport and Reactor Safety, (1978).

7. Duffin, W.J., Electricity and Magnetism, McGraw-Hill, Toronto, (1973).

8. Fujii, J., J. IEE Jap., 98B, 861 (1978).

9. Gardner, G.C., "Onset of Slugging in Horizontal Ducts", Int. J. of Multiphase Flow, 5, 201-209, (1979).

10. Johnson, R.L., "Effect of an Electric Field on Boiling Heat Transfer", AIAA, 6, 1456-1460, (1967).

11. Kordyban, E., "The Transition to Slug Flow in the Presence of Large Waves", Int. J. Multiphase Flow, 3, 603-607, (1977).

12. Kordyban, E.S., and Ranov, T., "Mechanism of Slug Formation in Horizontal Two-Phase Flow", Journal of Basic Engineering, December (1970).

13. Kronig, R., and Ashmann, G., Appl. Sci. Res. A1 (1949) 31.

14. Lamb, H., Hydrodynamics, 6th ed. Dover Publications, N.Y. (1945).

15. Levich, V.G., Physicochemical Hydrodynamics, Prentice-Hall, Englewood Cliff, N.J. (1962).

15. Lovenguth, R.L., and Hanesian, D., "Boiling Heat Transfer in the Presence of Nonuniform, Direct Current Electric Fields", Ind. Eng. Chem. Fundamentals, 10, 570-576, (1977).

16. Mandhane, J.M., Gregory, G.A., and Aziz, K., Int. J. of Multiphase Flow, 1, 537, (1974).

17. Markels, M., and Durfee, R.L., "The Effect of Applied Voltage on Boiling Heat Transfer", A.I.CH.E., January (1964).

18. Mascarenhas, S., "Thermodynamical Theory of Thermal Conduction of Dielectrics under Electric Fields", Il. Nuovo Cimento, V, (1957).

19. Takaka, Kubo, IEEE Jap. 1977 Meeting (1977).

20. Taitel, Y., Barnea, B., Shoham, O., "Flow Pattern Transition for Gas-Liquid Flow in Horizontal and Inclined Pipes", Int. J. Multiphase Flow, 6, 217-225 (1979).

21. Taitel, Y., and Dukler, A.E., "A Model For Predicting Flow Regime Transitions in Horizontal and Near Horizontal Gas-Liquid Flow", A.I.CH.E., 22, 47-54, (1976).

22. Wallis, G.B., and Dobson, J.E., "The Onset of Slugging in Horizontal Stratified Air-Water Flow", Int. J. Multiphase Flow, 1, 173-193 (1973).

23. Watabe, Kikudu, and Yokahuma, J. IEEE Jap. 99, 443 (1979).

24. Weisman, J., Duncan, D., Gibson, J., and Crawford, T., "Effects of Fluid Properties and Pipe Diameter on Two-Phase Flow Patterns in Horizontal Lines", Int. J. Multiphase Flow, 5, 437-462, (1979).

# APPENDIX 1

## List of Symbols Used in the Programs

AG - $A_G$, dimensionless gas area

AL - $A_L$, -dimensionless liquid area

BETA - $f_c$, for the slug and wavy transitions, and $P_E$ for the bubbly transition

CG - $C_G$, gas friction coefficient

CL - $C_L$, liquid friction coefficient

D - pipe internal diameter

DG - $D_G$, dimensionless gas hydraulic diameter

DL - $D_L$, dimensionless liquid hydraulic diameter

DT - pipe thickness

EPSO - $\varepsilon_o$, free space dielectric constant

EPS2 - $\varepsilon_2$, dielectric constant of water

FESQ - $F_E^2$, square of the electrical Froude number

G - g, gravitational acceleration

HL - $H_L$, dimensionless height of the liquid

M - power for gas friction coefficient (Eq,n 15)

N - power for liquid friction coefficient (Eq,n 15)

NUG - $\nu_G$, gas viscosity

NUL - $\nu_L$, liquid viscosity

REG1 - $Re_G$, gas Reynold s number

REL1 - $Re_L$, liquid Reynold s number

RHOG - $\rho_G$, gas density

RHOL - $\rho_L$, liquid density

S - sheltering coefficient

SG - $S_G$, gas perimeter

SI - $S_I$, gas-liquid interface perimeter

SL - $S_L$, liquid perimeter

UG - $U_G$, dimensionless gas velocity

UGS - $U_G^S$, specific gas velocity

UL - $U_L$, dimensionless liquid velocity

ULS - $U_L^S$, specific liquid velocity

V - voltage between electrodes

XSQH - $X^2$ (Eq'n 18)

# PROGRAM 1

## Transition from Stratified Smooth to Stratified Wavy Flow

```
      PROGRAM TST( INPUT, OUTPUT, TAPE5= INPUT, TAPE6=OUTPUT)
      REAL N, M, NUL, NUG
      DATA NUL/8.93E-7/, NUG/1.56E-5/, RHOL/997.07/, RHOG/1.185/,
     1D/.0190/, PI/3.1415927/
      DATA EPSO/8.8542E-12/, EPS2/72./, S/.01/
      DT=.0254/8.
      G=9.8
      READ*, V
       DIS=D+2.*DT
      WRITE(6,290) V, DIS
  290 FORMAT( 1H1, 30HTRANSITION TO WAVE FLOW AT V= , F7.1, 22H VOLTS AND
     1DISTANCE , F5.2, 21H M BETWEEN ELECTRODES)
      WRITE(6,300)
  300 FORMAT( 1H0, 7X, 3HULS, 9X, 3HUGS, 6X, 1HN, 5X, 1HM, 7X, 2HHL, 7X, 3HXSQ)
      CG=.046
      M=.2
      CL=16.
      N=1.
      REL1=2400.
      REG1=2400.
      DO 10 I=1,99
        HL=FLOAT( I)/100.
      BETA=(V**2)*EPSO*( 1.-1./EPS2)**2/(DIS-HL*D*( 1.-1./EPS2))**3
      X=2.*HL-1.
        AL=.25*( PI-ACOS( X)+X*SQRT( 1.-X**2))
        AG=.25*( ACOS( X)-X*SQRT( 1.-X**2))
        SL=PI-ACOS( X)
        SG=ACOS( X)
      SI=SQRT( 1.-X**2)
        UL=.25*PI/AL
        UG=.25*PI/AG
        DL=4.*AL/SL
        DG=4.*AG/(SI+SG)
```

```
      XSQH=AL*((UL*DL)**(N))*((UG*DG)**(-MD))*(UG**2)*(SG/AG+SI/AL+
     1SI/AG)/((UL**2)*SL)
      K=0
   15 CONTINUE
      K=K+1
      UGS=.1
      ULS=.0001
        J=0
   20 CONTINUE
        J=J+1
        GF=4.*NUL*(RHOL-RHOG)*G**2
        EF=2.*BETA*(UL*ULS)**3
        IF (EF.GT.GF) GO TO 70
        UGS1=SQRT((4.*NUL*(RHOL-RHOG)*G**2-2.*BETA*(UL*ULS)**3)/
     1  (S*RHOG*UL*ULS*UG**2))
       ULS1=(XSQH*CG*((UGS*D/NUG)**(-MD))*RHOG*(UGS**2)/(CL*((D/NUL)*
     1*(-N))*RHOL))**(1./(2.-N))
       DIFF1=ABS((ULS1-ULS)/ULS1)
       DIFF2=ABS((UGS1-UGS)/UGS1)
        ULS=ULS1
        UGS=UGS1
        IF (J.GT.300) GO TO 30
        IF (DIFF1.GT.0.001.OR.DIFF2.GT.0.001) GO TO 20
        DGT=DG*D
        UGT=UG*UGS
        REG=DGT*UGT/NUG
        DLT=DL*D
        ULT=UL*ULS
        REL=DLT*ULT/NUL
        DIFFRG=ABS(REG-REG1)
        DIFFRL=ABS(REL-REL1)
        IF (DIFFRG.LT.10.0.AND.DIFFRL.LT.10.) GO TO 40
        IF (REG.GT.2000.) GO TO 50
```

```
      CG=16.
      M=1.
      GO TO 55
   50 CG=.046
      M=.2
   55 CONTINUE
      IF (REL.GT.2000.) GO TO 60
      CL=16.
      N=1.
      GO TO 65
   60 CONTINUE
      CL=.046
      N=.2
   65 CONTINUE
      REG1=REG
      REL1=REL
      GO TO 15
   40 CONTINUE
      WRITE(6,310) ULS,UGS,N,M,HL,XSQH
  310 FORMAT(1H ,1X,F10.4,2X,F10.4,2X,F5.3,2X,F5.3,2X,F6.3,2X,F10.4)
      GO TO 10
   30 WRITE(6,330) HL
  330 FORMAT(1H ,35HCONVERGENCE IS NOT REACHED FOR HL= ,F6.4)
      GO TO 10
   70 WRITE(6,340)
  340 FORMAT(1H ,"WAVES OCCUR AT ZERO VELOCITY")
   10 CONTINUE
      STOP
      END
SSC       B3IIDGK   BRUNNER KS 81/08/25. 20.25.34.  PLOT   0
```

# PROGRAM 2

## Transition from Stratified to Slug Flow

```
      PROGRAM TST( INPUT,OUTPUT,TAPE5= INPUT,TAPE6=OUTPUT)
      REAL N,M,N1,M1,NUL,NUG
      DATA NUL/8.93E-7/,NUG/1.56E-5/,RHOL/997.07/,RHOG/1.185/,
     1D/.0190/,PI/3.1415927/
       DATA EPSO/8.8542E-12/,EPS2/80./
      DT=.0254/8.
      G=9.8
      READ*,V
      DIS=D+2.*DT
      WRITE(6,290) V,DIS
  290 FORMAT( 1H1,30HTRANSITION TO SLUG FLOW AT V= ,F7.1,22H VOLTS AND
     1DISTANCE ,F5.2,21H M BETWEEN ELECTRODES)
      WRITE(6,300)
  300 FORMAT( 1H0,7X,3HULS,9X,3HUGS,6X,1HN,5X,1HM,7X,2HHL,7X,3HXSQ,9X,
     14HFESQ)
      DO 10 I=1,99
      HL=FLOAT( I)/100.
      BETA=( 1.-1./EPS2)**2*( V**2)*EPSO/(( D-D*HL*( 1.-1./EPS2))**3)
      X=2.*HL-1.
      AG=.25*( ACOS( X)-X*SQRT( 1.-X**2))
      UG=.25*PI/AG
      FESQ=(( 1.-HL)**2)*AG/( UG**2*SQRT( 1.-X**2))
      UGS=SQRT( FESQ*D*(( RHOL-RHOG)*G-BETA)/RHOG)
   40 CONTINUE
      J=0
      X=2.*HL-1.
      AL=.25*( PI-ACOS( X)+X*SQRT( 1.-X**2))
      AG=.25*( ACOS( X)-X*SQRT( 1.-X**2))
      SL=PI-ACOS( X)
      SG=ACOS( X)
      SI=SQRT( 1.-X**2)
      UL=.25*PI/AL
      UG=.25*PI/AG
```

```
      DL=4.*AL/SL
      DG=4.*AG/(SG+SI)
      DGT=DG*D
      UGT=UG*UGS
      REG=DGT*UGT/NUG
      IF (REG.GT.2000.) GO TO 41
      CG=16.
      M=1.
      GO TO 50
   41 CONTINUE
      CG=.046
      M=.2
   50 CONTINUE
      CL=.046
      N=.2
   51 CONTINUE
      J=J+1
      XSQH=AL*((UL*DL)**(N))*((UG*DG)**(-M))*(UG**2)*(SG/AG+SI/AL+
     1SI/AG)/((UL**2)*SL)
      ULS=(XSQH*CC*((UGS*D/NUG)**(-M))*RHOG*(UGS**2)/(CL*((D/NUL)*
     1*(-N))*RHOL))**(1./(2.-N))
      ULT=UL*ULS
      DLT=DL*D
      REL=DLT*ULT/NUL
      IF (J.EQ.2) GO TO 60
      IF (REL.GT.2000.) GO TO 60
      CL=16.
      N=1.
      GO TO 51
   60 CONTINUE
      WRITE(6,310) ULS,UGS,N,M,HL,XSQH,FESQ
  310 FORMAT(1H ,1X,F10.4,2X,F10.4,2X,F5.3,2X,F5.3,2X,F6.3,2X,F10.4,2X
     1F10.4)
```

```
      10 CONTINUE
         STOP
         END
SSC      B3IIDJA   BRUNNER KS 81/08/25. 20.50.02.  PLOT   0
```

PROGRAM 3

Transition from Slug to Bubbly flow

```
      DG=4.*AG/(SI+SG)
     XSQH=AL*((UL*DL)**(N))*((UC*DG)**(-MD))*(UC**2)*(SG/AG+SI/AL+
    1SI/AG)/((UL**2)*SL)
      K=0
15  CONTINUE
      K=K+1
        FL=DL*UL*D/NUL
        GF=G*(RHOL-RHOG)*AG*D/SI
        ULS=(4.*(FL**(-N))*(GF+PE)/(CL*RHOL*(UL**2)))**(1./(2.+N))
        UGS=(CL*((ULS*D/NUL)**(-N))*RHOL*(ULS**2)/(CG*XSQH*((D/NUG)
     1    **(-MD))*RHOG))**(1./(2.-MD))
        DGT=DG*D
        UGT=UG*UGS
        REC=DGT*UGT/NUG
        DLT=DL*D
        ULT=UL*ULS
        REL=DLT*ULT/NUL
        DIFFRG=ABS(REC-REC1)
        DIFFRL=ABS(REL-REL1)
        IF (DIFFRG.LT.10.0.AND.DIFFRL.LT.10.) GO TO 40
        IF (REC.GT.2000.) GO TO 50
        CG=16.
        M=1.
        GO TO 55
50  CG=.046
        M=.2
55    CONTINUE
        IF (REL.GT.2000.) GO TO 60
        CL=16.
        N=1.
        GO TO 65
60  CONTINUE
        CL=.046
```

```
      N=.2
   65 CONTINUE
      REG1=REG
      REL1=REL
      GO TO 15
   40 CONTINUE
      WRITE(6,310) ULS,UGS,N,M,HL,XSQH
  310 FORMAT(1H ,1X,F10.4,2X,F10.4,2X,F5.3,2X,F5.3,2X,F6.3,2X,F10.4)
      GO TO 10
   30 WRITE(6,330) HL
  330 FORMAT(1H ,35HCONVERGENCE IS NOT REACHED FOR HL= ,F6.4)
   10 CONTINUE
      STOP
      END
```

SSC B3IIDIX BRUNNER KS 81/08/25. 20.49.30. PLOT 0